DEPARTMENT OF OCEANOGRAPHY
COLLEGE OF SCIENCES
OLD DOMINION UNIVERSITY
NORFOLK, VIRGINIA 23529

DTIC
ELECTE
JUN 27 1991
S
C
D

Technical Report No. 91-6

MESOSCALE CHARACTERISTICS AND THE ROLE OF DEFORMATION ON OCEAN DYNAMICS

By

Albert D. Kirwan Jr., Principal Investigator

Final Report
For the period 1 October 1987 to 31 January 1989

Prepared for
Office of Naval Research
800 N Quincy Street
Arlington, Virginia 22217-5000

Under
ONR Contract N00014-88-K-0203
Dr. Thomas Kinder, Scientific Officer

Submitted by the
Old Dominion University Research Foundation
P.O. Box 6369
Norfolk, Virginia 23508-0369

1991

DISCLAIMER NOTICE
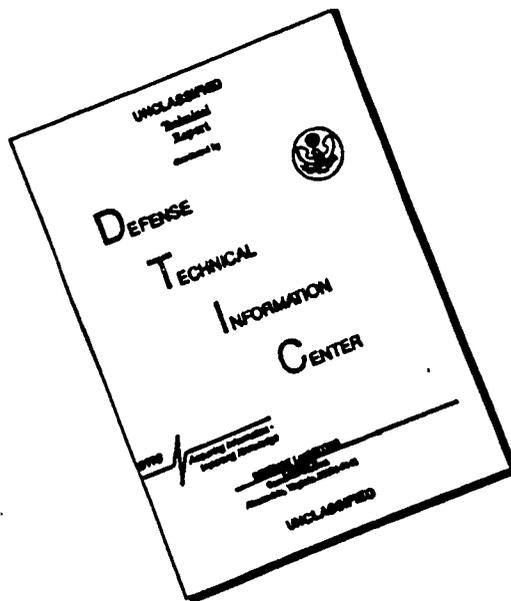
THIS DOCUMENT IS BEST QUALITY AVAILABLE. THE COPY FURNISHED TO DTIC CONTAINED A SIGNIFICANT NUMBER OF PAGES WHICH DO NOT REPRODUCE LEGIBLY.

OCEANOGRAPHY
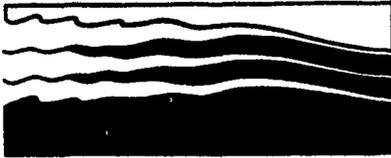
OLD DOMINION UNIVERSITY

*Department of Oceanography
Old Dominion University
Norfolk, Virginia 23529-0276
(804) 683-4285
Fax (804) 683-5303*

June 5, 1991

Chief of Naval Research
c/o Dr. Thomas Kinder
Office of Naval Research
800 N Quincy Street
Arlington, VA 22217-5000

Dear Sir/Madam:

This letter constitutes the revised final report for ONR contract N00014-88-K-0203 awarded to Old Dominion University for the period October 1, 1987 though January 31, 1989. The original final report was submitted to the Office of Naval Research as part of a renewal proposal.

The bulk of the research activities conducted under this contract consisted of basic research on ocean flow dynamics as it pertains to the prediction of ocean motion. During the contract period, three papers describing aspects of the research were published in the adjudicated scientific literature. These papers are:

1. "Genesis of the Gulf of Mexico Ring as Determined from Kinematic Analysis," *J. Geophys. Res.*, 92(C11), 11727-11740, 1987.

2. "Observed and Simulated Kinematic Properties of Loop Current Rings," *J. Geophys. Res.*, 93(C2), 1189-1198, 1988.

3. "Notes on the Cluster Method for Interpreting Relative Motions," *J. Geophys. Res.*, 93(C8), 9337-9339, 1988.

In addition to these papers, the results of the research were reported at the 1988 Liege Colloquium on Ocean Hydrodynamics, Mesoscale/Synoptic Coherence in Geophysical Turbulence..

As a part of the research effort, the funds were used to support William Indest, a Ph.D. graduate student in the Department of Oceanography.

I am grateful to the Office of Naval Research for continued support for this research.

Respectfully,

A. D. Kirwan, Jr.
Samuel L. and Fay M. Slover
Chair of Oceanography

Genesis of a Gulf of Mexico Ring as Determined From Kinematic Analyses

JAMES K. LEWIS

Science Applications International Corporation, College Station, Texas

A. D. KIRWAN, JR.[1]

University of South Florida, Department of Marine Science, St. Petersburg

The kinematics of the Loop Current are studied using trajectories of drifters in the Gulf of Mexico during mid-June through September 1985. One of the drifters was in the Loop Current proper, while other drifters were in two recently shed Loop Current rings. The drifter in the Loop Current showed strong anticyclonic motion during the study period. This Loop Current anticyclone first began off the northwest coast of Cuba. It rapidly moved northward into the Gulf of Mexico as a ring pinched off from the Loop Current. Analysis of the Loop Current drifter motion showed that the anticyclone became an integral part of the Loop Current, taking on many of the characteristics of the most recently shed ring. The results of the analysis suggest a process by which Loop Current rings can be generated. Apparently, this mechanism can cause the Loop Current to become reconfigured in 2-3 months for beginning the process of ring separation.

1. INTRODUCTION

The shedding of Loop Current rings has a major impact on processes in the central and western Gulf of Mexico. These large anticyclones transport a tremendous amount of momentum, heat, and salt across the gulf, all the way to the Mexican coast [*Elliot*, 1982; *Kirwan et al.*, 1984; *Lewis and Kirwan*, 1985]. In order to consider balances of momentum, mass, and heat within the Gulf of Mexico, it is important to have some idea of the characteristics of the kinematics of the Loop Current, including how often a ring may be pinched off.

During June 1985, an attempt was made to put an Argos drifter into the Loop Current as a ring was pinching off. However, the ring did not totally disconnect from the Loop Current, and the drifter ended up spending approximately 3 months in the Loop Current proper. The drifter exited the Gulf of Mexico (GOM) through the Florida Straits in September 1985 (Figure 1, drifter 3354). Fortunately, a second drifter (3378, Figure 1) was placed in the ring in July 1985. Together, these two Lagrangian data sets provide a unique view of the motion of the Loop Current while it is in the process of shedding a ring. They provide special insight into Loop Current kinematics as this system extends northward, as well as the kinematics of a Loop Current ring. Finally, we comment on the existence of a third anticyclone in the GOM. The eddy was discovered serendipitously as a third drifter became entrained in its flow field and circled around the eddy all the way to the Mexican coast (G. Forristall, personal communication, 1986). This eddy has been referred to as Ghost Eddy because there had been no previous indication of its existence prior to the first of August 1985. Its general motion and extent during August and September 1985 is shown in Figure 1.

The following analysis is obtained from the movement of drifters 3354 and 3378 as well as concurrent sea surface temperature (SST) data and XBT data. These, along with the presence and location of Ghost Eddy, suggest a new process by which an anticyclonic vortex is formed that can eventually become a Loop Current ring. The original mechanism for spinning up the vortex appears to be the lateral sharing stresses caused by the Loop Current off the northwest coast of Cuba.

A detailed description of the kinematic characteristics of the Loop Current and the ring is provided by an analysis of the drifter paths. This analysis gives us the time histories of the rotation rate, eccentricity and orientation of the ellipses of the trajectories, swirl velocities, and movement of the centers of rotation. A comparison is made of the kinematics of the Loop Current as determined by drifter 3354 during the time it coexisted with a ring. The latter is designated by drifter 3378. The comparison of the last part of drifter 3354 (before it exited the GOM) with the first month of ring 3378 provides an interesting contrast between the motion characteristics of a northern extension of the Loop Current before and after it pinches off to become a ring.

2. PATH DATA

The path data used in this study are the position data of the drifters with Argos identification numbers 3354 and 3378. The GOM ring that was seeded by drifter 3378 will be referred to as ring 3378. References to drifter 3354 will indicate a reference to the Loop Current proper. Drifter 3378 was drogued by a weighted 200-m line, while drifter 3354 was drogued by a window shade drogue at 100 m.

Drifter 3354 was seeded at 25.9°N, 87.9°W on June 18, 1985. The drifter immediately moved southeastward ~525 km and reached 23.2°N, 83.7°W by June 29, 1985. At this point the drifter became entrained in a westward, anticyclonic flow field with a center of rotation at about 24°N, 85.5°W. After two rotations (into mid-August) the drifter suddenly moved northwestward and made three additional rotations centered at about 25.5°N, 86.5°W. The drifter then left this flow pattern in
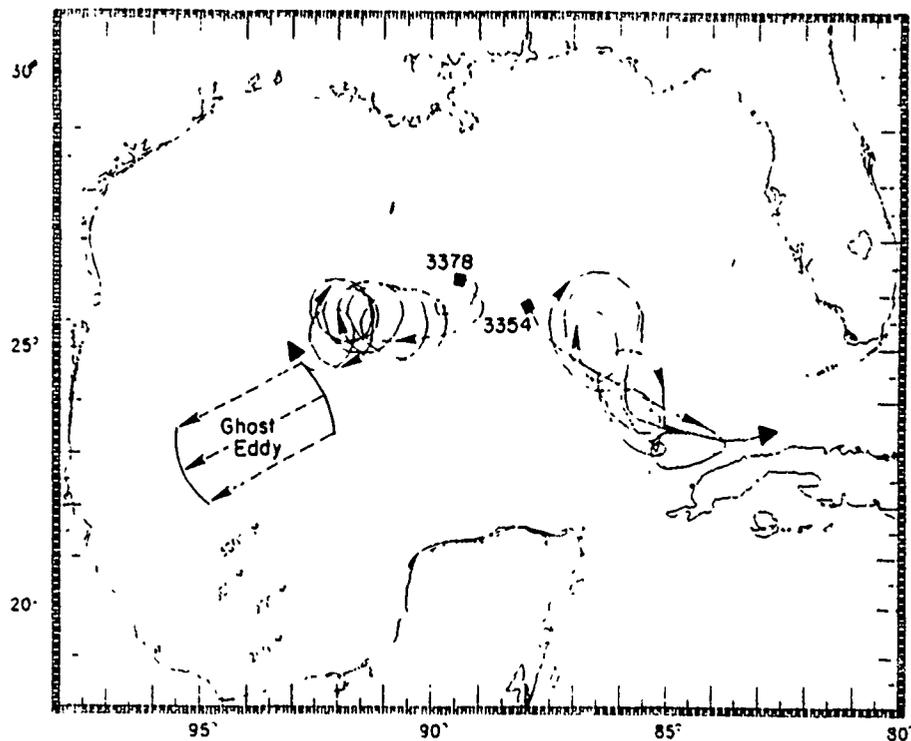
Fig. 1. Trajectories of drifter 3354 from mid-June through mid-September 1985 and of drifter 3378 from mid-July through September 1985. Also shown is the location of Ghost Eddy during August and September 1985. Squares denote the beginning positions of the drifter trajectories and triangles denote the end positions.

mid-September 1985 and exited the GOM through the Flori- da Straits.

Drifter 3378 was seeded in ring 3378 at 26.4 N, 89.3 W on July 18, 1985 By that time, the ring had totally separated from the Loop Current As shown in Figure 1, ring 3378 slowly moved westward, reaching approximately the 91 W meridian by mid-August Recall that after mid-August, the Loop Current (as determined by drifter 3354) moved north-

westward and remained there until at least mid-September. During that same 30-day period, ring 3378 continued moving westward, reaching to the 92.5′ W meridian.

The offshore industry launched a drifter in June 1985 which eventually became entrained in the flow field of Ghost Eddy. At the beginning of August 1985, this ring was centered at 23.5 N, 93 W (Figure 1). The ring gradually moved southwest- ward across the deepest portion of the GOM. By the end of September 1985, Ghost Eddy was still strongly rotating at 23 N, 94.5 W.

3. TEMPERATURE DATA

A number of XBT data sets were collected in the eastern GOM during May-September 1985 (Table 1). These data pro- vide indications of the location and the structure of the Loop Current and ring 3378. In addition, weekly SST contour charts are available for the entire gulf. Some of these SST data are presented here, but unfortunately little in the way of ther- mal structure can be picked out since the SST gradients are small in the GOM during the study period (summer and early fall).

Cruise tracks for the period May 26-31, 1985, are shown in Figure 2a. The resulting XBT data are shown in Figures 2b -2d. These data were collected before ring 3378 was shed, and the edges of the Loop Current (maximum horizontal tem- perature gradients) indicated by the XBT data are shown in Figure 2a. (Smaller slopes of the isotherms were taken as an indication that the transects were crossing the Loop Current edge at an angle, and some of the edges were thus drawn at a 45 angle to the cruise track.) It appears that the Loop Cur-

TABLE 1   Listing of Cruises During Which XBT Data Were Collected in the Central and Eastern Gulf of Mexico

Vessel	Date (1985)
E. M. Queeny	May 7 ?
M/V Nestor I	May 10 11
M V Stena Hispania	May 17 18
E. M. Queeny	May 26 27
M/V Stena Hispania	May 27 28
M/V Stena Hispania	May 30-31
E M. Queeny	June 7 8
L. M. Queeny	June 13-14
M/V Stena Hispania	June 26-28
M/V Stena Hispania	June 29-30
E. M. Queeny	July 1-2
R/V Suncoaster	July 9 22
M V Nat Co 6	July 16-19
M/V Stena Hispania	July 16-17
E. M. Queeny	July 31 to Aug. 1
M/V Stena Hispania	Aug. 16-18
M V Ambassador	Sept. 4 5
M. V Ambassador	Sept. 13 14
M/V Ambassador	Sept 24-25

Fig. 2. (a) Cruise tracks for XBT data collected during May 26–31, 1985. The arrows denote the flow at the edges of the Loop Current based on the vertical temperature structure shown in (b) temperature data from the E. M. Queeny cruise, May 26–27, 1985. (c) temperature data from the Stena Hispania cruise, May 27–28, 1985, and (d) temperature data from the Stena Hispania cruise, May 30 31, 1985.

rent was flowing northward on the east side of the Yucatan Straits, swirled westward and around the region where ring 3378 would be spawned, and then turned northeastward before exiting the GOM.

As previously mentioned, drifter 3354 was deployed in the northward extension of the Loop Current during mid-June 1985. The trajectory of 3354 during June 18–24, 1985, is plotted on the corresponding GOM SST chart in Figure 3. As

indicated by the trajectory (and to some degree by the SST data), ring 3378 had obviously not separated from the Loop Current during this period. The return flow from the area of the northward extension appears to be mostly southeastward, toward the northern coast of Cuba.

Three XBT data sets were collected during June 26 to July 2, 1985 (Figure 4), and the temperature profiles are shown in Figures 4b–4d. The outline of ring 3378 is quite distinct in
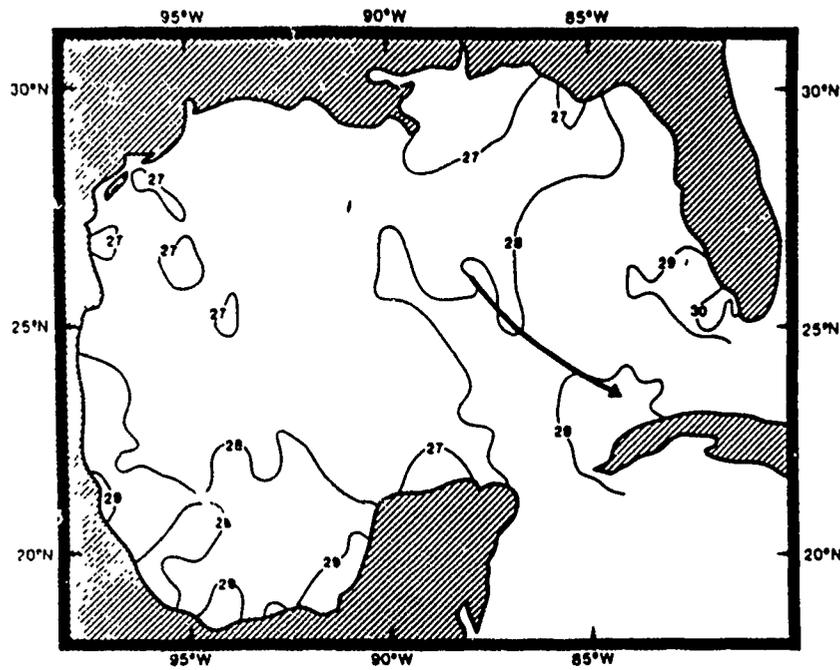
Fig. 3. Trajectory of drifter 3354 and SST data for June 18-24, 1985.

Figures 4b and 4c, while the Loop Current can be seen to extend to 25 N in Figure 4d. These data would seem to imply that ring 3378 is still connected to the Loop Current. The SST data for June 29 to July 5, 1985, along with the associated trajectory of drifter 3354 are shown in Figure 5. The outlines of the ring and the Loop Current from the XBT data in Figure 4a are also shown, and we see some of the rotational characteristics within the Loop Current from the path of drifter 3354. The rotation near the Cuban coast continued into mid-July.
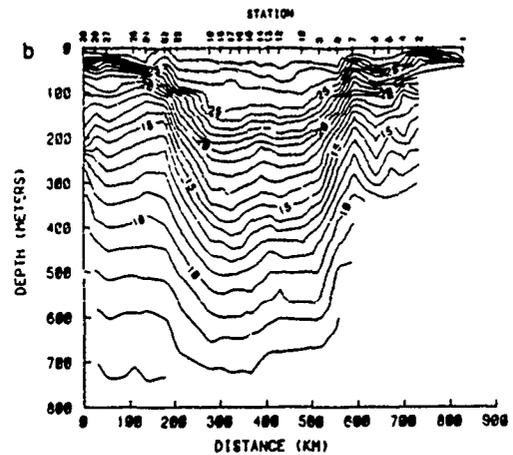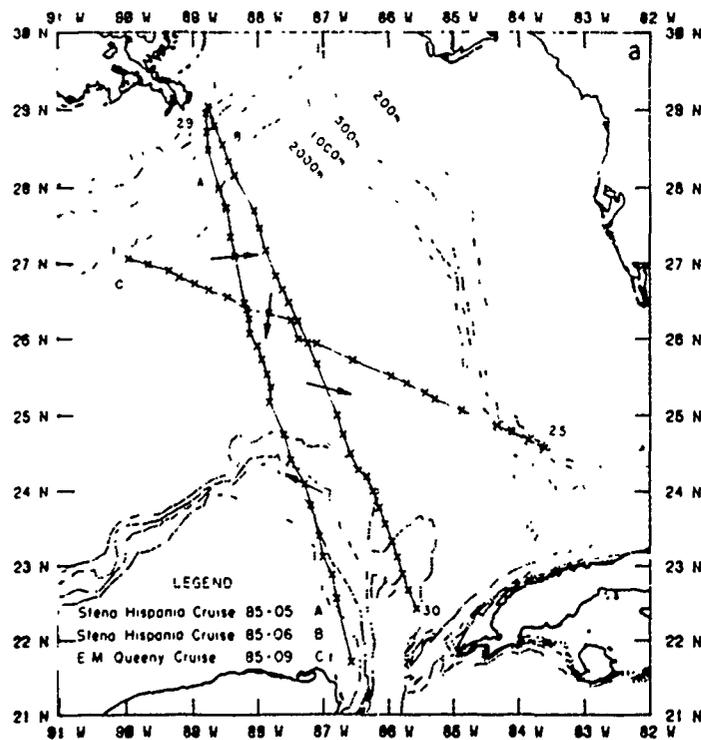
Fig. 4. (a) Cruise tracks for XBT data collected during June 26 to July 2, 1985. The arrows denote the flow at the edges of the Loop Current based on the vertical temperature structure shown in (b) temperature data from the Stena Hispania cruise, June 26-28, 1985, (c) temperature data from the Stena Hispania cruise, June 29-30, 1985, and (d) temperature data from the L. M. Queeny cruise, July 1-2, 1985.
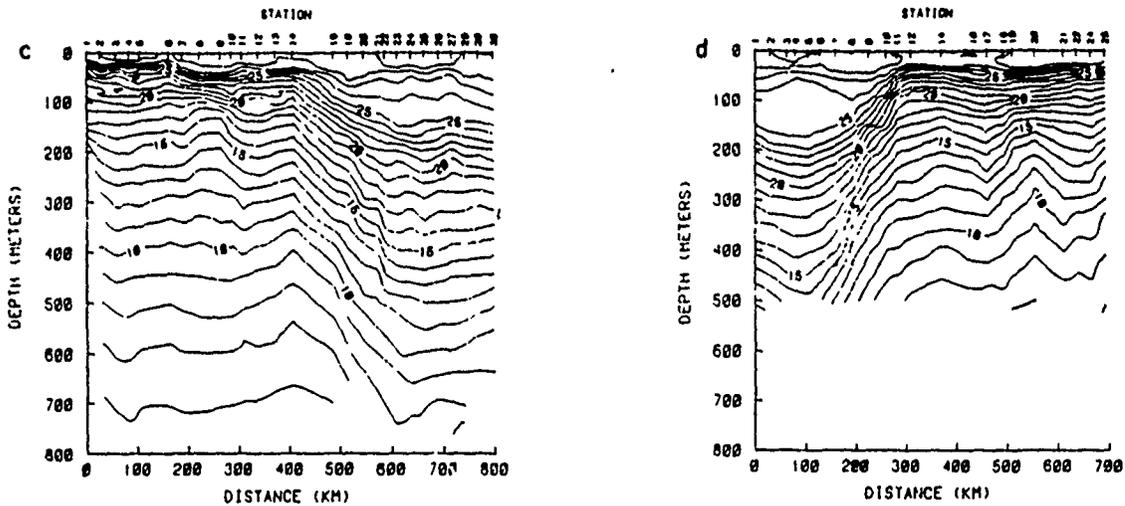
Fig. 4 (continued)

During July 16–19, 1985, two XBT data sets were collected (Figure 6) which distinctly show that ring 3378 had separated from the Loop Current. The SST contours for the same period are shown in Figure 7. There is no surface signature of ring 3378, although its rotation is well delineated by the trajectory of drifter 3378. As for the Loop Current, Figure 7 shows that the rotational feature within the current had reached the northern edge of the current, about 25° N.

Both the Loop Current and ring 3378 continued to rotate anticyclonically through August 1985. An XBT data set collected on August 16–18, 1985 (Figure 8) indicates that the Loop Current had extended northward to 26.6 N. Looking at the SST map for August 12–19, 1985 (Figure 9), we see that ring 3378 and the Loop Current were rotating at about the same latitude, 25.5 N. By mid-September, the sea surface had cooled sufficiently in the eastern GOM so that the northern

extension of the Loop Current is readily defined (Figure 10). The trajectories for this period of time show ring 3378 strongly rotating but drifter 3354 leaving the rotational feature of the Loop Current along the eastern side of a 28°C tongue of water. The following week's SST chart (Figure 11) shows the 28 °C tongue reaching up to 27.5°N, while drifter 3354 moved toward the Florida Straits along the northern coast of Cuba. Ring 3378 was still rotating with a center at about 25.5 N, 92 W.

4. KINEMATIC ANALYSES

The trajectory data were used to calculate various kinematic parameters of the flow field. The methodology outlined by Kirwan et al. [1984, 1987] for geophysical fluids was used in these calculations. (For more details, see Kirwan et al. [1987].) Although Kirwan et al. [1984] used a 100-hour low-
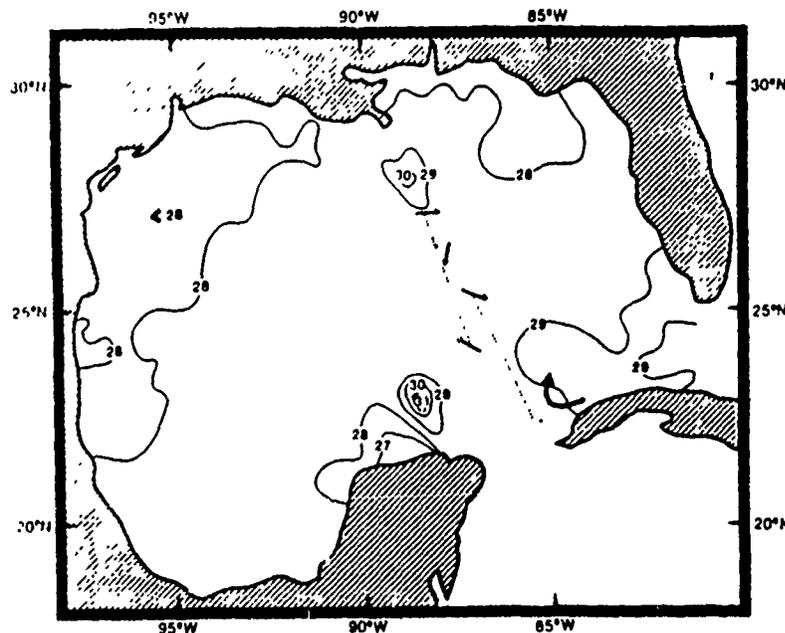
Fig. 5. Trajectory of drifter 3354 (large arrow) and SST data (C) for June 29 to July 5, 1985. Shorter arrows denote the flow at the edges of the Loop Current while dotted lines indicate the locations of Loop Current waters (based on XBT data)
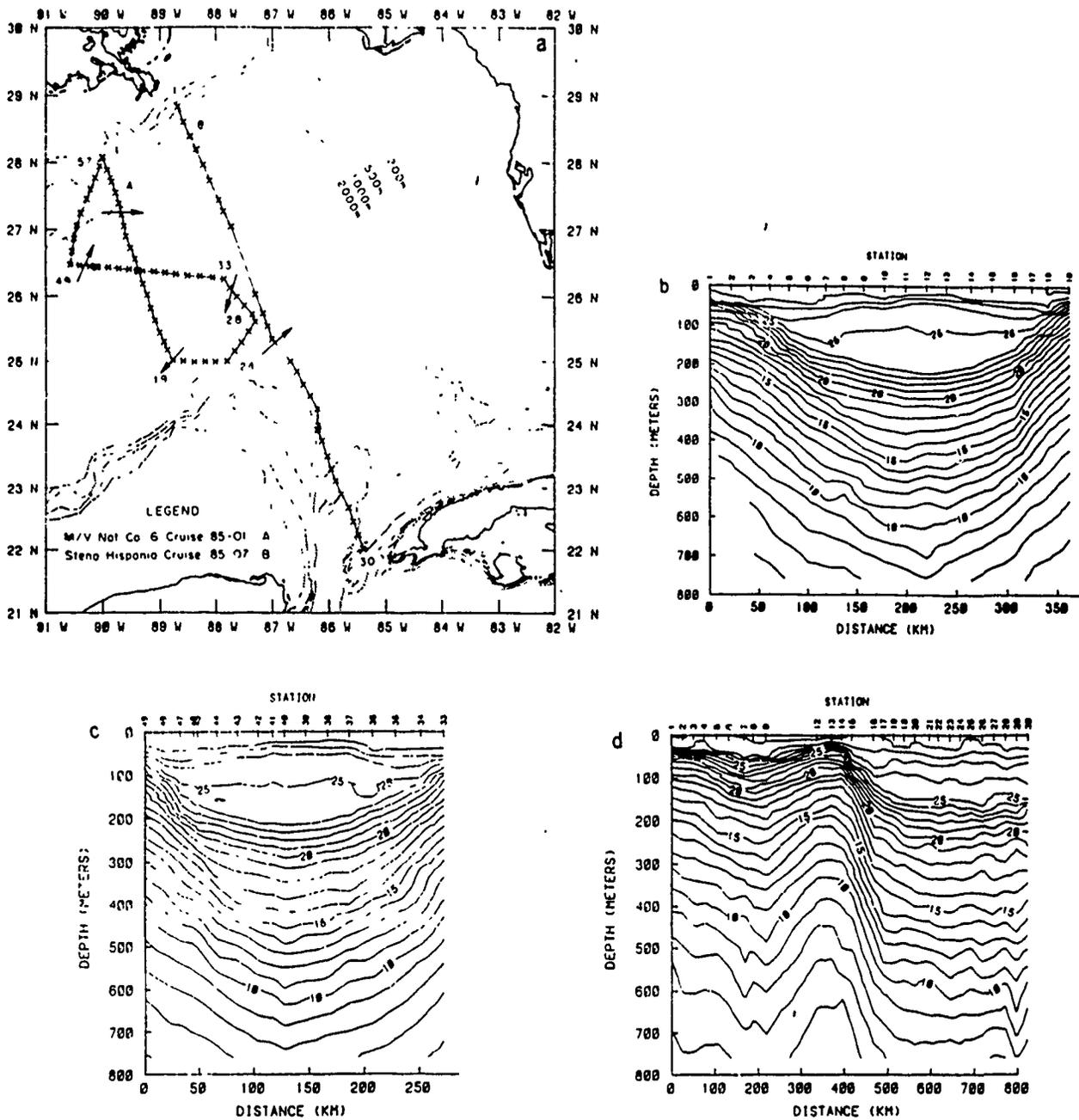
Fig. 6. (a) Cruise tracks for XBT data collected during July 16–19, 1985. The arrows denote the flow at the edges of the Loop Current and ring based on the vertical temperature structure shown in (b) and (c) both temperature data from the M, V Nat Co 6 cruise, July 16–19, 1985, and (d) temperature data from the Stena Hispania cruise, July 16–17, 1985.

pass filter in making their calculations for a ring in the western GOM, it was found in this study that such a filter was not sufficient to remove higher-frequency fluctuations recorded by drifter 3354. As a result, we used a 164-hour (half power point) low-pass filter on the velocity data of the drifters. We then calculated the period of rotation, the ellipticity, the orientation, and the velocity about the translation ring center (swirl velocity) as seen by drifters 3354 and 3378.

Loop Current Kinematics

The observed (filtered) Loop Current velocities as seen by drifter 3354 are shown in Figure 12. The speed fluctuates in magnitude from 15 to 80 cm/s, and there are minimums at the

beginning of the record and during Julian days 210–225. It was during days 220–230 that drifter 3354 moved northwestward, an apparent rapid northward extension of the Loop Current. The swirl velocity associated with the rotation of the Loop Current is shown in Figure 13. These magnitudes also vary from 15 to 80 cm/s.

The extent of water involved with the northward movement of the Loop Current is indicated by Figure 14, which shows the time history of the distances from the drifter to the center of rotation. Prior to the northwest movement, the maximum radius of the rotation as seen by the drifter was 85 km. After the northwest movement the radius increased up to 100 km.

The rotational frequency of the Loop Current is shown in
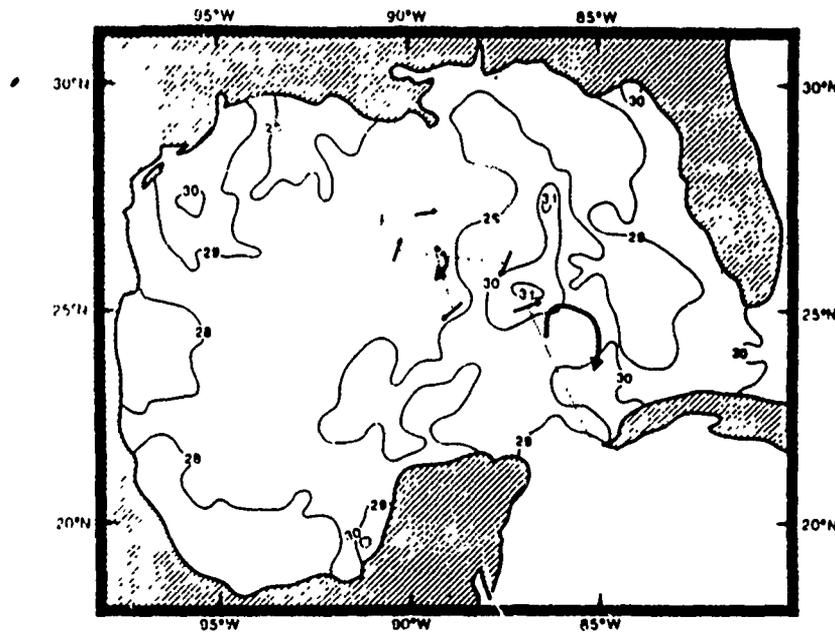
Fig. 7 Trajectories of drifters 3354 (solid large arrow) and 3378 (dashed large arrow) and SST data (C) for July 16–23, 1985. Shorter arrows denote the flow at the edges of the Loop Current, while dotted lines indicate the locations of Loop Current waters (based on XBT data)

Figure 15. (For the calculation of this term, see *Kirwan et al.* [1984]) Figure 15 shows a general decrease and then increase in frequency, with a minimum occurring right before the northwestward extension of the water mass. As the water moved northwest, the mean period of rotation decreased from about 13 days to approximately 10.5 days. If we compare Figures 14 and 15, we see that longer periods tend to be associated with larger radii.
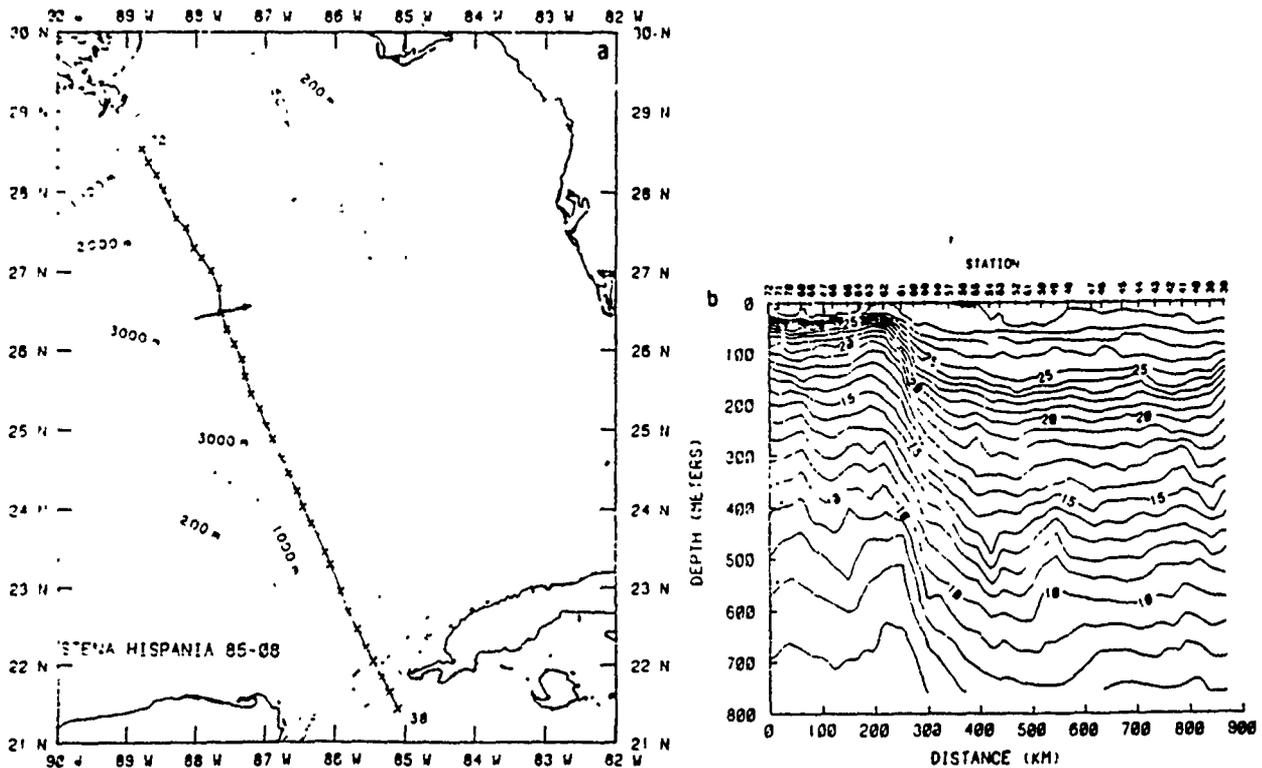
Fig. 8 (a) Cruise track for XBT data collected during August 16–18, 1985. The arrow denotes the flow at the edge of the Loop Current based on the vertical temperature structure shown in (b) temperature data from the *Siena Hispania* cruise, August 16–18, 1985
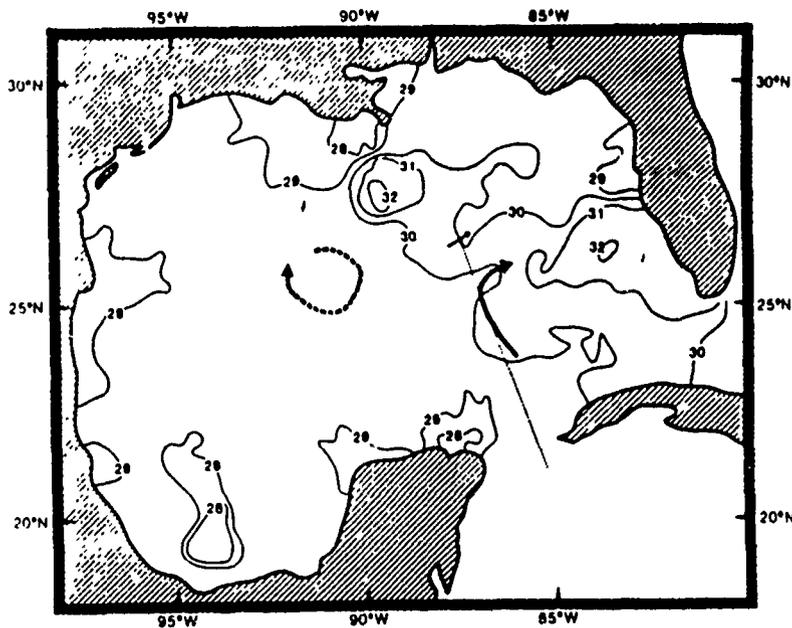
Fig. 9. Trajectories of drifters 3354 (solid large arrow) and 3378 (dashed large arrow) and SST data (°C) for August 12 19, 1985. Shorter arrow denotes the flow at the edge of the Loop Current, while dotted lines indicate the location of Loop Current waters (based on XBT data).

As for the shape of the field of rotation, we use eccentricity e, defined as the major axis length divided by the minor axis length. Also, we calculate the northeast orientation of the major axis, and both of these variables are shown in Figure 16. The flow field starts out rather elliptical ($e - 1.75$) but becomes more circular by day 250 ($e = 1.4$). The elliptical orientation was mostly east west at first but eventually became more northwest southeast.

Kinematics of Ring 3378

The filtered velocities of ring 3378 are shown in Figure 17. The magnitudes of these oscillations are relatively large, up to ~85 cm/s with a minimum of about 50 cm/s. The swirl speeds are shown in Figure 18, and we see here an initial increase from 20 to 75 cm/s followed by a decrease to about 50 to 60 cm/s. These variations in swirl magnitude coincide with vari-
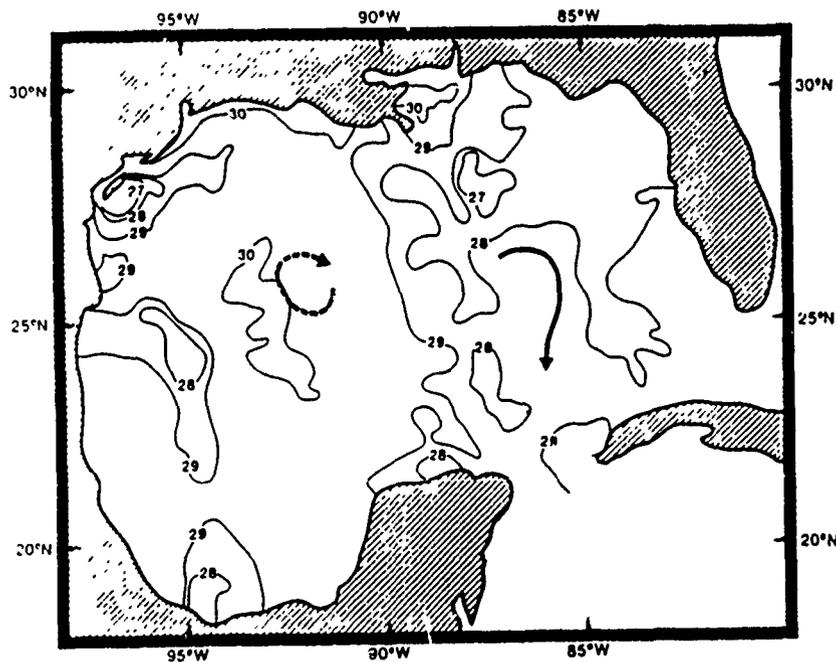
Fig. 10. Trajectories of drifters 3354 (solid large arrow) and 3378 (dashed large arrow) and SST data (°C) for September 10 17, 1985.
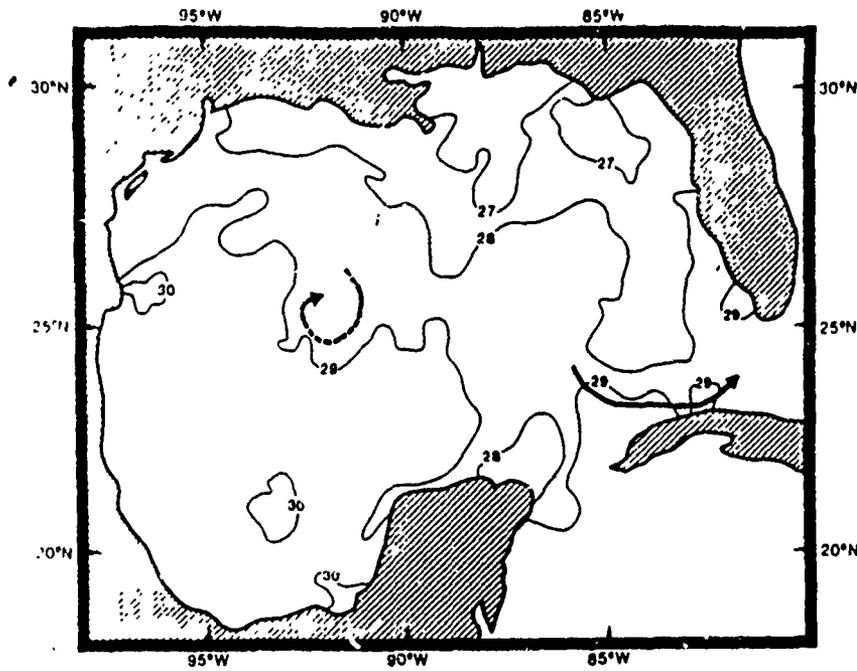
Fig. 11. Trajectories of drifters 3354 (solid large arrow) and 3378 (dashed large arrow) and SST data (°C) for September 17-24, 1985.

ations in the size of the circle of rotation (Figure 11). Figure 19 quantifies the distances from the center of rotation, with a maximum radius of 95 km.

The rotation frequency of ring 3378 is shown in Figure 20. The initial minimum in frequency (~0.11 ¹) is followed by an increase to about 0.14⁻¹. From about day 220 and on, the rotational frequency of ring 3378 gradually decreased, with the period of rotation increasing from about 8 days to about 9 days.

Considering the shape, the data indicate that the ring was initially rather elliptical (Figure 21). Within two rotation periods this eccentricity decreased somewhat, with the ring becoming almost circular. The results shown in Figure 21 imply that the initial ellipse orientation was mostly east/west. This orientation did not seem to change significantly as the ring became more circular.

5. DISCUSSION

The classical concept of Loop Current processes is one in which part of the Gulf Stream at first flows directly from the Yucatan Straits to the Florida Straits. Within this flow field,
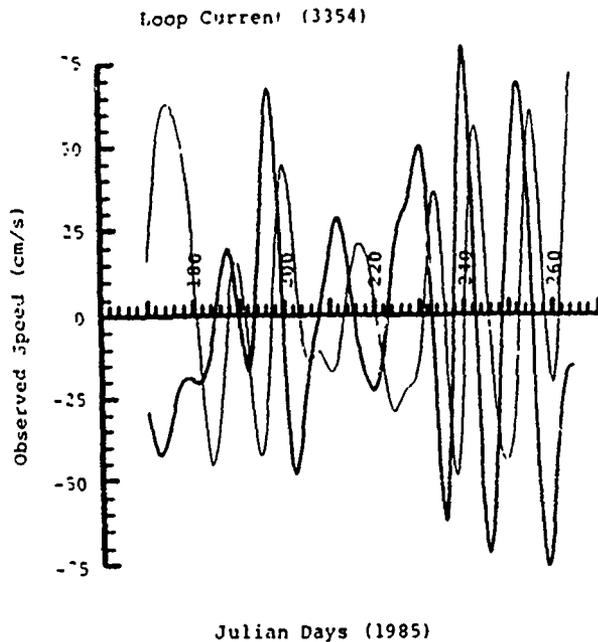
Fig. 12. Time histories of the filtered observed speed components for drifter 3354. The light curve is the east/west speed, and the darker curve is the north/south speed.
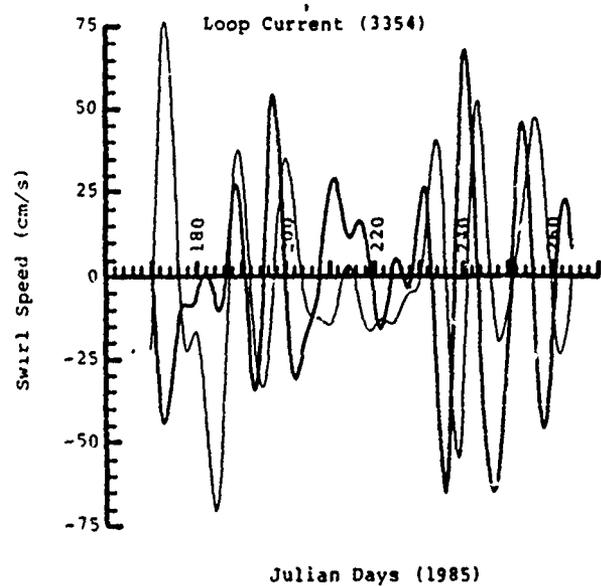
Fig. 13. Time histories of the swirl speed components about the center of rotation for the Loop Current. The light curve is the east/west speed, and the darker curve is the north/south speed.
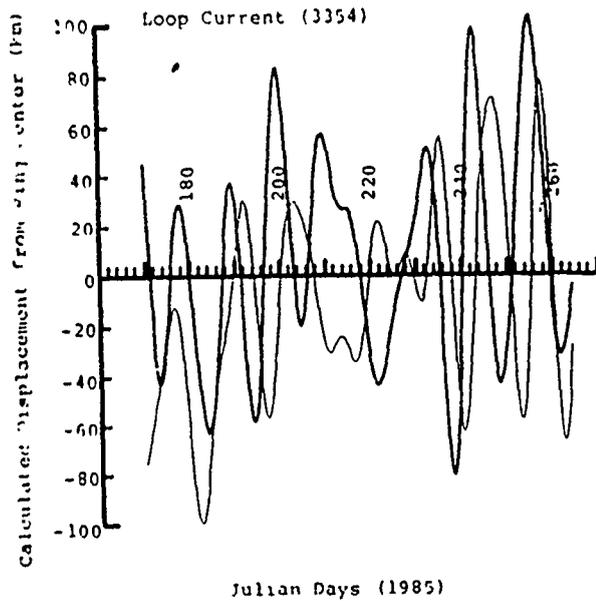
Fig. 14 Time histories of the east/west (light curve) and north/south (darker curve) distances of drifter 3.54 from the center of rotation in the Loop Current

Fig. 16. Time histories of the Loop Current eccentricity (asterisks) and orientation of major axis (dashed lines). For the flow field orientation, north is in the positive e direction, and east is in the positive time direction.

instabilities exist which result in meandering of the Loop Current [*Hurlburt and Thompson*, 1980]. As the sizes of the meanders increase and reach northward, it is generally believed that the flow field wraps back onto itself and "shorts" across the stream of flow part of the flow would still go northward around the Loop Current extension, while the remainder of the flow would take the more direct, southerly route to the Florida Straits This is analogous to other geophysical phenomena, such as the creation of ox-bow lakes by meandering rivers. Finally, as the curvature of the flow reaches its maximum, more of the Loop Current flow takes the southerly route, and a GOM ring is eventually pinched off.

The interesting point indicated by the data presented here is the closed anticyclonic flow within the Loop Current immedi-

ately after ring 3378 was pinched off. Also, the trajectory of drifter 3354 reveals that this rotational feature initially existed off the coast of Cuba. It has been shown in numerical studies that the flow of the Loop Current can itself create an anticyclonic flow field off the northwestern coast of Cuba [*Thompson*, 1986]. The northward flow west of the tip of Cuba along with the southeasterly flow along the north central coast of Cuba will obviously produce negative vorticity off Cuba's northwestern shore. Such an anticyclonic flow has been documented by a number of hydrographic surveys [e.g., *Nowlin and McLellan*, 1967; *Cochrane*, 1972]. Using hydrographic data, *Hofmann and Worley* [1986] estimated the depth
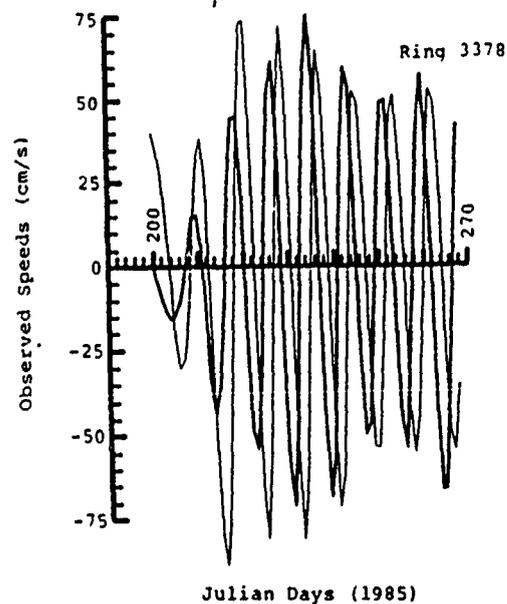
Fig. 17. Time histories of the filtered observed speed components for ring 3378. The light curve is the east/west speed, and the darker curve is the north/south speed.

Fig. 15. Time history of the rotational frequency within the Loop Current.

Ring 3378

Julian Days (1985)
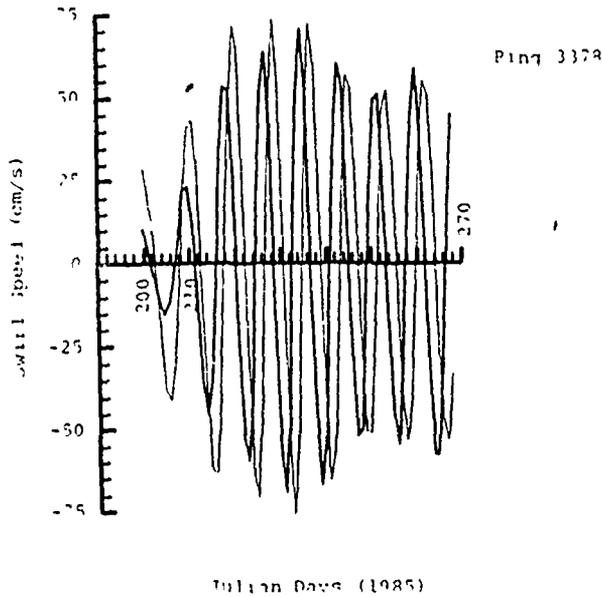
Fig. 18 Time histories of the swirl speed components about the center of rotation for ring 3378 The light curve is the east west speed, and the darker curve is the north south speed

of this Cuban eddy to be ~800 m with a current magnitude of 10-25 cm s, in good agreement with the data from this study (Figure 12) Also, data show that the temperature and salinity characteristics of GOM rings and the Cuban eddy are practically identical [McLellan, 1960, Elliot, 1982]

The Cuban eddy appears to be the flow field in which drifter 3354 initially became entrained. The drifter trajectory indicates that this flow field moved slightly northwest while ring 3378 was still connected to the Loop Current. But it was only shortly after ring 3378 pinched off that this anticyclone pushed more northwesterly, to about 26 5 N Figures 10 and 11 indicate that after this final push (late August 1985), the rotational field became an integral component of the Loop Current. Thus the data in this case imply that the kernels of Loop Current rings may come from waters off the northwest coast of Cuba.

Fig 20 Time history of the rotational frequency of ring 3378

An example of a modeled ring pinch-off in the GOM is shown in Figures 22 and 23 [from Wallcraft, 1986]. On day 63 (Figure 22) the model shows a configuration similar to that when drifter 3354 was seeded. The ring is well defined as the northern extension of the Loop Current, but it has not completely pinched off Note that there does exist a hint of anticyclonic motion off the northwestern coast of Cuba. By day 153 (3 months later) the model shows the ring free of the Loop Current. Moreover, the anticyclone off Cuba is larger and much better defined. However, the model shows the northern edge of the Loop Current extending to only 26 N, whereas XBT and drifter data presented here show an extension to 27 N in a similar time period (3 months).

It is not until after 9 months before the Loop Current in this simulation pushes northward again in the process of

Ring 3378

Julian Days (1985)

Fig 19 Time histories of the east west (light curve) and north south (darker curve) distances of drifter 3378 from the center of rotation of ring 3378

Ring 3378

Julian Days (1985)
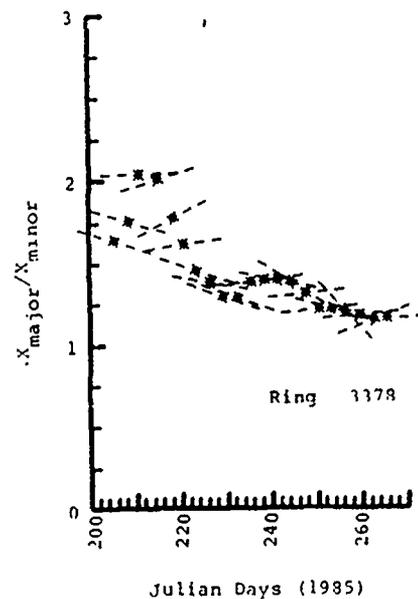
Fig. 21 Time histories of the eccentricity (asterisks) and major axis orientation (dashed lines) for ring 3378 For the flow field orientation, north is in the positive e direction, and east is in the positive time direction.

LAYER 1 CURRENTS

DATE = 063/1969
G OF MEXICO 20132 2 13 0

31N

05 M/S

MAX PLOTTED SPEED = 0.95 (M/SEC)

18N

80W
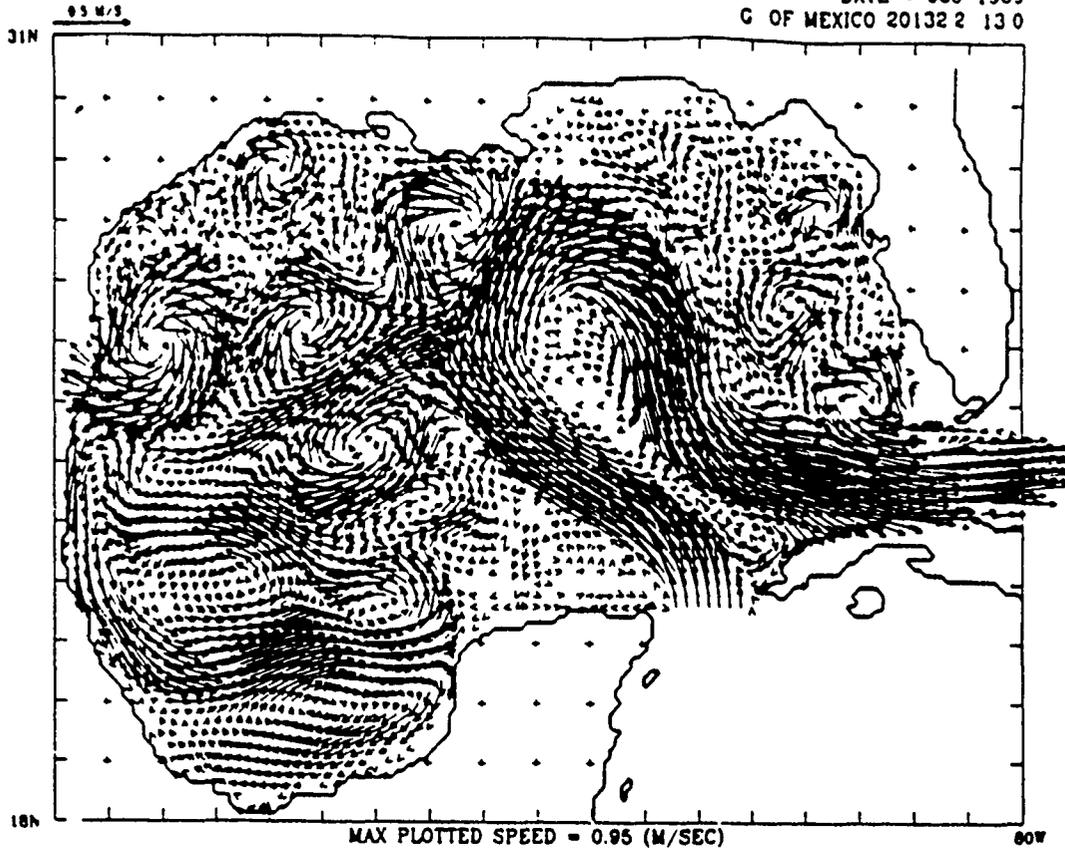
LAYER 1 CURRENTS

DATE = 153/1969
G OF MEXICO 20132 2: 13.0

31N

05 M/S

MAX PLOTTED SPEED = 0.98 (M/SEC)

18N

98W

80W
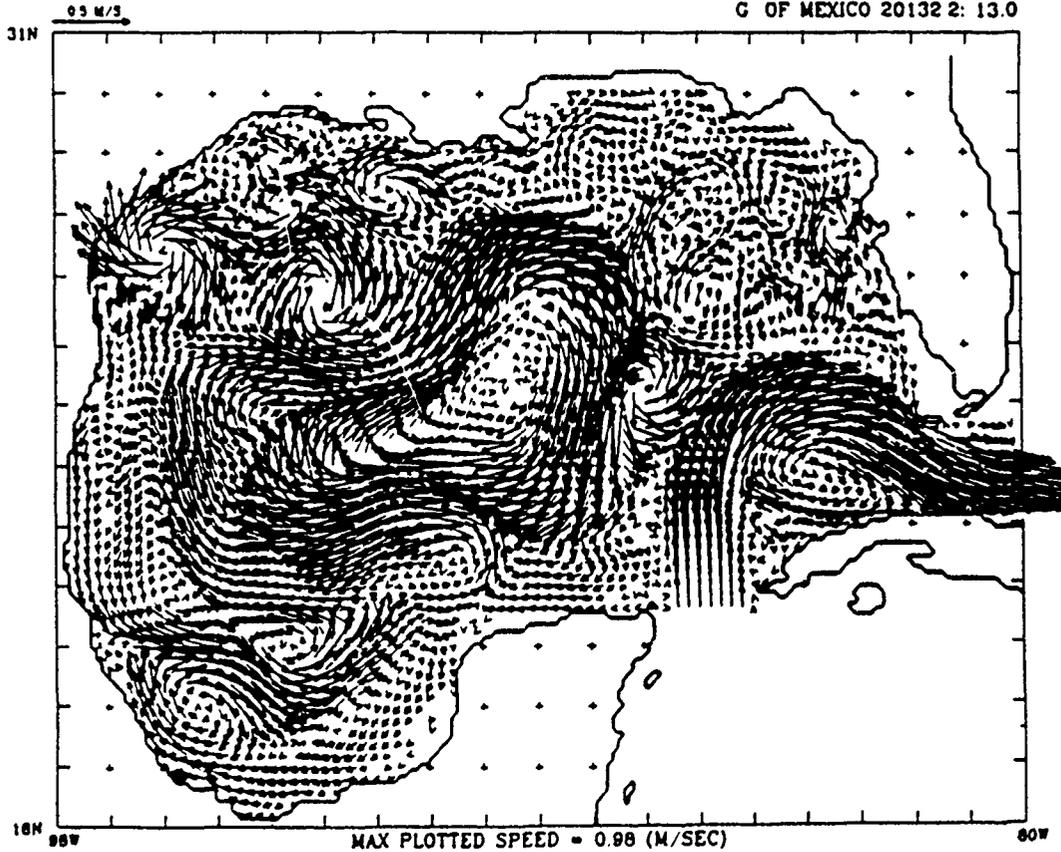
Fig 22   Upper layer water velocities from a model of the Gulf of Mexico for days 63 (top) and 153 (bottom) [from Wallcraft, 1986]. The top layer is 200 m deep

LAYER 1 CURRENTS

DATE = 243/1969
G OF MEXICO 20132 2 13 0

31N

0 9 M/S

MAX PLOTTED SPEED = 0.94 (M/SEC)

18N 98W

80W

LAYER 1 CURRENTS

DATE = 333/1969
G OF MEXICO 20132.2 13.0

31N

0 9 M/S

MAX PLOTTED SPEED = 1.10 (M/SEC)

18N 98W

80W
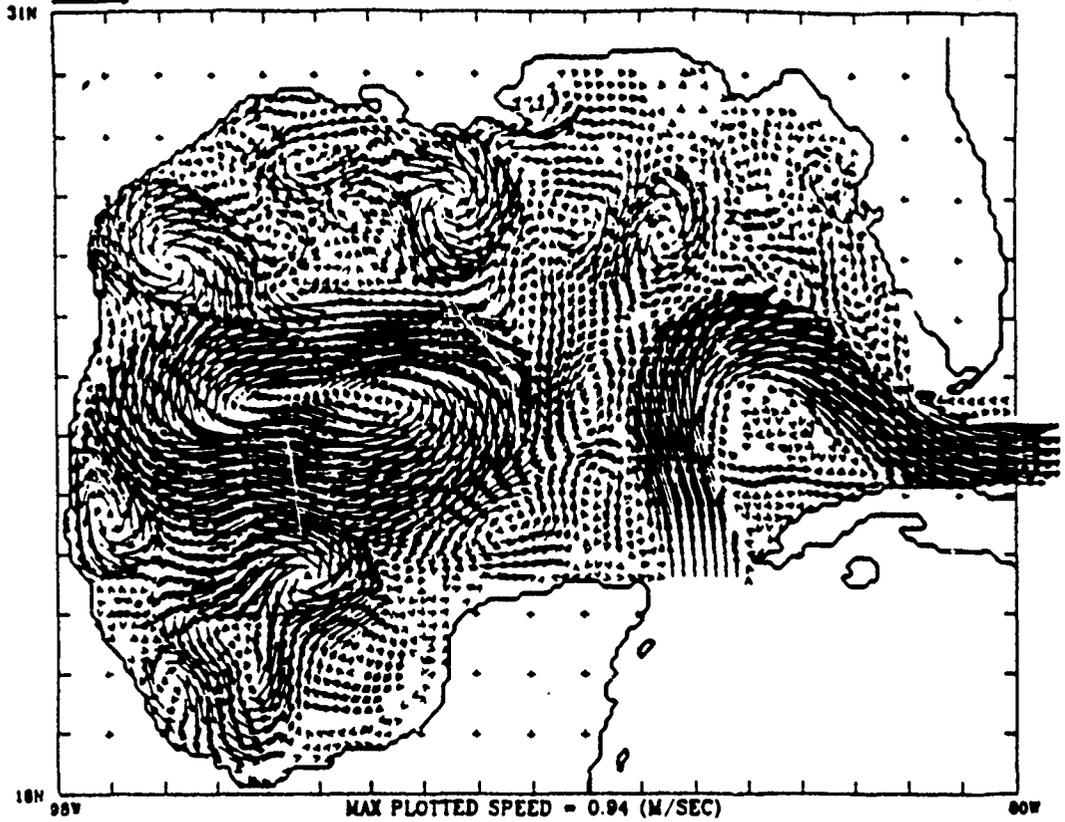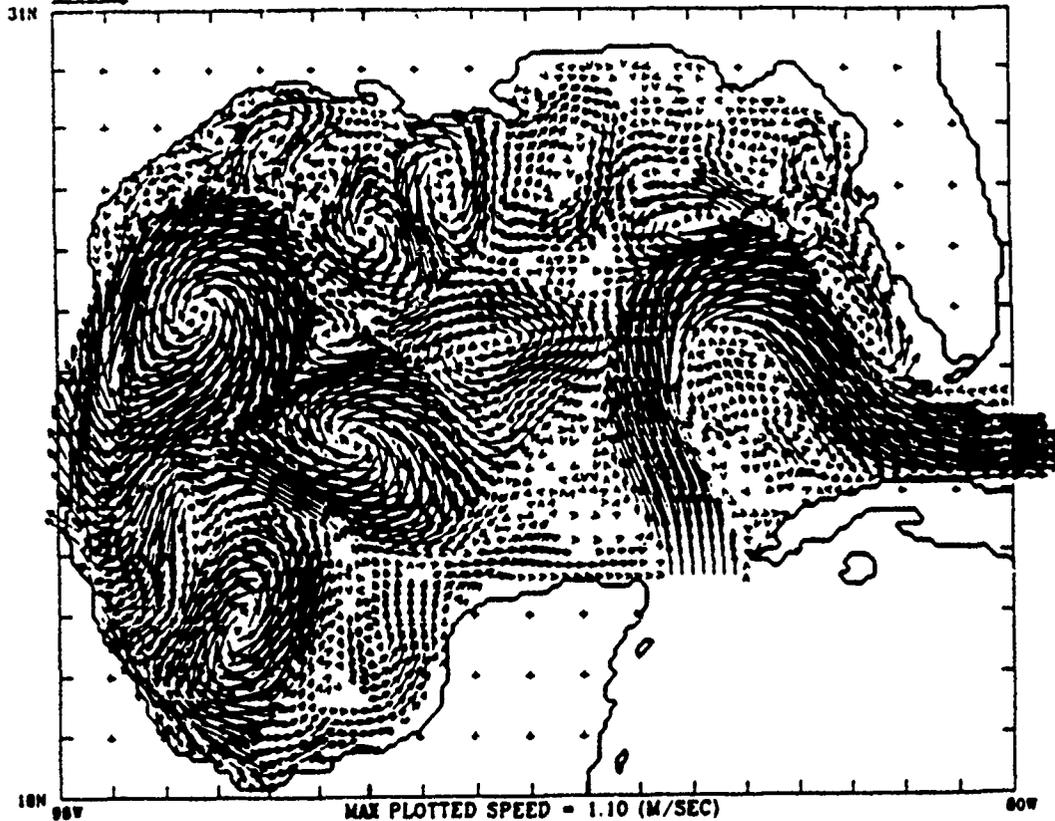
Fig. 23. Upper layer water velocities from a model of the Gulf of Mexico for days 243 (top) and 333 (bottom) [from Wallcraft, 1986]. The top layer is 200 m deep.

pinching off another ring (Figure 23). By this time, the anti-
cyclone that had been spun up by the Loop Current has lost
its identity (day 223 Figure 23) Thus the process as deter-
mined from the trajectories of drifter 3354 is different from this
particular simulation in two major ways. First, the Loop Cur-
rent ... moved northwestward to 27 N in 2.5 months
... a value of 10 months for such model
... Second, this rapid extension was accompanied by
... circulation vortex originally generated off the coast
of Cuba. However, in other simulations with no deep in-flow
through the Yucatan Straits, significant Loop Current pene-
trations can occur in 40 days Clearly, this is a phenomena
that requires further study

Loop Current Versus Ring Kinematics

Drifters 3354 and 3378 were both in the GOM during
Julian days 199-264, 1985. However, the initial variations of
the kinematic parameters of ring 3378 (Figures 17-21) all indi-
cate an adjustment period from days 199-220 during which
time the drifter (with its 200-m weighted line) found an appro-
priate orbit within the ring Thus we compare the ring and
Loop Current kinematics from day 225 to day 264. At the
beginning of this time period the Loop Current was rotating
with a period of about 10.5 days, while ring 3378 had a period
of ~ 8.2 days. The orientations of the ellipses of rotation (Fig-
ures 16 and 21) were quite similar (generally east-west), but the
Loop Current was slightly more elliptical (e = 1.5) than ring
3378 (e = 1.25)

The swirl speeds and the radii of revolution for the drifters
in both anticyclones were quite similar for days 225-264· 80
cm s for the swirl speeds, and ~ 90 km for the radii relative to
the ring center. Interestingly, both anticyclones experienced
longer periods of rotation for smaller distances from the center
of rotation.

Kinematics Before and After a Ring Detachment

We now turn to the kinematics of the Loop Current at its
most northerly extension (Julian days 230-264) and the kin-
ematics of ring 3378 soon after it broke free from the Loop
Current (Julian days 225-235) Keeping in mind that these
data represent two different anticyclonic phenomena, how
typical are the GOM rings before and after they break off
from the Loop Current?

The similarities between the two sets of kinematics are con-
siderable. First, the magnitudes of the swirl speeds and of the
radii are practically identical. Moreover, their elliptical orien-
tations are both northwest/southeast. The Loop Current was
slightly more elliptical than ring 3378, but one might expect
such a difference in ellipticity seeing that an anticyclone still
attached to the Loop Current is a "captured" phenomena,
while a detached ring is an isolated vortex. The similarities of
the anticyclones plus their close periods of rotation imply that
the basic kinematic characteristics of GOM rings can be es-
tablished as the Loop Current pushes northwestward off the
shore of Cuba.

Summary

The scenario implied here is one in which the essence of the
ring is established off the northwest coast of Cuba, develops in
deeper waters off the coastline, and then takes on its final
characteristics shortly after the previous ring completely de-
taches from the Loop Current.

The implication of such a mechanism is that of time scales
One is not required to wait until instabilities in the flow field
grow large enough to produce a closed rotational feature. The
data here show that a new Loop Current rotational feature
can be well established even before the previous ring has to-
tally pinched off. It was established that ring 3378 was de-
tached from the Loop Current by mid-July 1985. Yet it was
seen that the new rotational structure had moved to latitude
26.5°N by the beginning of September 1985 Thus the Loop
Current was reconfigured for another ring separation only 1.5
months after the previous ring separation. Elliot [1982] docu-
mented three ring separations in a 12-month period using
hydrographic data. The presence of Ghost Eddy along with
ring 3378 implies a similar separation rate. Model studies
[e.g., Hurlburt and Thompson, 1980; Thompson, 1986; Wall-
craft, 1986] report separation rates ranging from 4 to 18
months, depending upon the type of instability involved.

REFERENCES

Cochrane, J D., Separation of an anticyclone and subsequent devel-
opments in the Loop Current (1969), in *Contributions on the Physi-
cal Oceanography of the Gulf of Mexico*, edited by L. R. A Capurro
and J. L. Reid pp 91 106, Guif Publishing, Houston, Tex., 1972
Elliot, B A., Anticyclonic rings in the Gulf of Mexico, *J Phys Ocean-
ogr. 12*, 1292 1309, 1982
Hofmann, E E., and S J. Worley, An investigation of the circulation
of the Gulf of Mexico, *J Geophys. Res. 91*(C12), 14,221-14,236,
1986
Hurlburt, H. E., and J. D. Thompson, A numerical study of Loop
Current intrusions and eddy shedding, *J Phys. Oceanogr. 10*,
1611-1651, 1980.
Kirwan, A. D., Jr., W. J. Merrell, Jr., J K. Lew, R E. Whitaker, and
R. Legeckis, A model for the analysis of drifter data with an appli-
cation to a warm core ring in the Gulf of Mexico, *J Geophys. Res.
89*(C3), 3425-3438, 1984.
Kirwan, A. D., Jr., J. K Lewis, A. W. Indest, P Reinersman, and I
Quintero, Observed and simulated kinematic properties of Loop
Current rings, *J. Geophys. Res.*, in press, 1987.
Lewis, J. K., and A. D. Kirwan, Some observations of ring topogra-
phy and ring-ring interactions in the Gulf of Mexico, *J Geophys
Res., 90*(C5), 9017-9028, 1985.
McLellan, H. J., The waters of the Gulf of Mexico as observed in 1958
and 1959, *Tech. Rep. 60-14T*, 17 pp., Dep. of Oceanogr, College
Station, Tex, 1960.
Nowlin, W. D., Jr., and H J. McLellan, A characterization of the Gulf
of Mexico waters in winter, *J. Mar. Res., 25*, 24 59, 1967.
Thompson, J. D., Altimeter data and geoid error in mesoscale ocean
prediction: Some results from a primitive equation model, *J Geo-
phys. Res., 91*(C2), 2401 2417, 1986.
Wallcraft, A. J., Gulf of Mexico circulation modeling study, annual
progress report· Year 2, report to Miner Manage Serv., 94 pp.,
JAYCOR, Vienna, Va., 1986.

A. D. Kirwan, Jr., Department of Oceanography, Old Dominion
University, Norfolk, VA 23508.
J. K Lewis, Science Applications International Corp., 1304
Deacon, College Station, TX 77840.

Observed and Simulated Kinematic Properties of Loop Current Rings

A. D. KIRWAN, JR.,[1,2] J. K. LEWIS,[3] A. W. INDEST,[4] P. REINERSMAN,[1] AND I. QUINTERO[1]

Two rings, shed by the Loop Current in 1980 and 1982, were observed for several months by satellite-tracked drifters to migrate across the Gulf of Mexico. The drifter path data have been inverted to obtain estimates of the paths of the centers of the two rings, ring shape, and the swirl velocities. Three drifters were deployed in the 1980 ring, and the analysis of that data set establishes the variability of the above kinematic estimates for one ring. A comparison of the analysis of data from both rings provides some idea on inter-ring variability. Both rings impacted the Mexican continental slope at about 22.8°N, 95 5'W After a brief adjustment period, both rings reestablished and maintained a vortex character for several months in the slope region while migrating slowly to the north. The paths of the centers of the two rings along the slope are virtually identical. The same analysis routine was applied to some simulated drifter data obtained from the Hurlburt and Thompson (1980) Gulf of Mexico primitive equation model. In the midgulf, the agreement between the observed rings and the simulated ring is good, although the former showed stronger interaction with the continental slope topography and/or circulation than was seen in the latter. Along the slope, the model ring kinematic characteristics were in extraordinary agreement with the observations.

1. INTRODUCTION

The circulation of the Gulf of Mexico has been the subject of a surprising amount of theoretical and observational studies. From the turn of the century [Sweitzer, 1898] until 1973 [Austin, 1955; Nowlin and McClellan, 1967; Nowlin, 1972], the emphasis was on analyses of hydrographic data. These studies established the presence of poorly defined, but quasi-permanent, anticyclonic signatures in the central part of the gulf.

Since 1973, the emphasis has shifted from qualitative descriptions of the hydrography to attempts at quantifying dynamical mechanisms associated with the anticyclonic structures. Sturges and Blaha [1976] and Blaha and Sturges [1978] proposed that the western gulf circulation was the result of the balance of wind stress curl and planetary vorticity, i.e., a mini–western boundary current effect in the Gulf of Mexico. Elliot [1979, 1982] disputed this, noting that this balance was not generally achieved if synoptic wind data on a fine scale were used His work also gave more credence to the earlier idea of Ichiye [1962] that the anticyclonic features were in fact rings that had been shed by the Loop Current in the eastern gulf. Kirwan et al. [1984a] substantiated this hypothesis by tracking the migration of a ring shed by the Loop Current across the gulf to the continental shelf off of Mexico.

In a companion paper, Kirwan et al. [1984b] assessed the translation velocities, local vorticity, deformation rates, and shape of the ring as it propagated across the gulf. The analyses of the three drifters that were in the ring simultaneously showed generally good agreement of these properties. The results also are in general qualitative agreement with the nu-

merical simulations from the general circulation model (GCM) of Hurlburt and Thompson [1980], hereinafter referred to as HT.

Is the qualitative agreement between GCM calculations and one particular ring fortuitous or the result of deterministic dynamics? We examine this question with observations from two different rings along with simulated data from the HT model. Specifically, we compare in detail kinematic properties such as the movement of ring centers, ring translation and swirl velocities, and ring shapes from 1980–1981, 1982–1983, and simulations from the HT GCM.

The analysis routine used to determine these kinematic properties is an improved version of that reported by Kirwan et al. [1984b]. The routine inverts Lagrangian path data to obtain the desired kinematic properties. Unlike the earlier study, the present routine emphasizes ring shape and translation. Also, considerably better time resolution on parameter estimates can be made with the new routine. Some details are given below and in the appendix. The internal consistency of the analysis routine is being assessed separately with simulated data from the HT GCM.

The following observed data were utilized in this study. These come from two rings which occurred in 1980–1981 and 1982–1983. We have reported previously on the former [see Kirwan et al., 1984a, b] using the more primitive analysis routine. That ring had three drifters in it simultaneously, and so our re-analysis provides some indication of intraring variability along with some indication of the consistency of the analysis routine. Only a descriptive analysis of the latter ring, which had only one drifter, has been reported before [Lewis and Kirwan, 1985]. Comparison of these two rings provides some measure of inter-ring variability.

These observed data are compared with simulated Lagrangian data from the HT GCM. This model was a two-layer (lower layer active) nonlinear primitive equation model of the Gulf of Mexico with realistic bottom topography. The grid spacing for the calculations used here was 10 km. The simulated path was obtained by advecting a parcel at each model time step (4 hours) to a new position given by the product of the velocity vector at the current position of the parcel and the time step. Since the position of the parcel was rarely at a grid point, it was usually necessary to interpolate the velocity vector from surrounding grid points. These calculations were kindly performed by A. Wallcraft.

[1]Department of Marine Sciences, University of South Florida, Saint Petersburg.

[2]Now at Department of Oceanography, Old Dominion University, Norfolk, Virginia.

[3]Science Applications International Corporation, College Station, Texas.

[4]Department of Oceanography, Old Dominion University, Norfolk, Virginia.

Both the observations and the simulations track appropriate rings for many months. During this time, the real and simulated rings move from the midgulf region with fairly flat topography in excess of 3000 m to the continental slope off of Mexico This area of interest is depicted in Figure 1. In the midgulf region, ring translations are governed essentially by Rossby wave dynamics, and so one expects them to move west-southwest But along the slope, interactions of the ring with bottom topography become important. Since the dynamics in these two geographic regions are so different, we have performed separate analyses for the rings in the two regions.
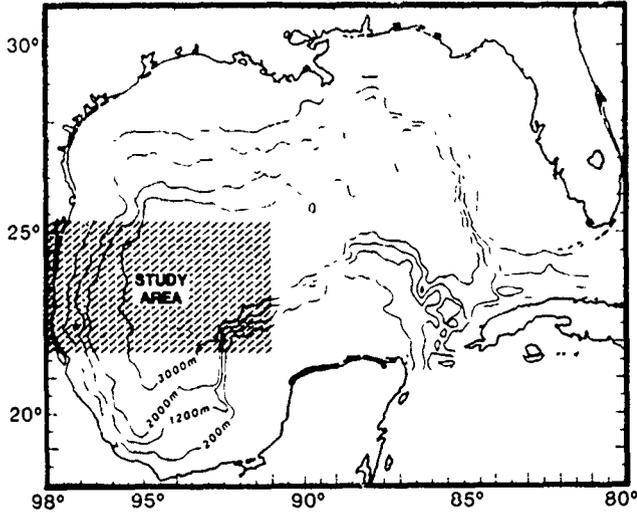
Fig 1   Depiction of the area in which the observed and simulated Loop Current rings are studied

2. ANALYSIS PROCEDURE

The observations used in this study are the positions of the Polar Research Laboratory drifters with Argos identifications 1598, 1599, 1600, and 3374. Kirwan et al. [1984a, b] reported on the analysis of 1598, 1599, and 1600, which were deployed simultaneously in November 1980. Position data from these three drifters are analyzed to establish the variability within a ring. Intraring variability is assessed by comparing the analysis performed on the three drifters in the 1980-1981 ring with that of drifter 3374, which was deployed in the 1982-1983 ring. Each drifter was the standard Polar Research Laboratory buoy drogued by a 200-m thermistor line. No thermistor data are available from any of these units.

The analysis procedure utilizes a parametric kinematic model discussed by Kirwan et al. [1984b] for inferring the translation and swirl velocities as well as the vorticity, horizontal divergence, and deformation rates. This model was first proposed by Okubo [1970] to describe small-scale motion about flow singularities. Kirwan [1984] showed that same model can be applied to larger scales if the model parameters are constant along a parcel path.

The model assumes that the swirl velocity is given as a linear function of the distance from a local flow center. Here the local parcel flow center will be referred to as the "ring center" or some times "orbit-determined center". This terminology is dictated only by the nature of the available data.

Fherl [1981] has pointed out that this center may not coincide with an "Eulerian" center. (We interpret this as a center of mass.) Smith and Reid [1982] have developed a general formalism for studying the centers of the distribution on any property, for example, mass, potential energy, kinetic energy or enstrophy. In general, these centers do not coincide, nor do their propagation velocities. Establishing the relations between these various centers for Gulf of Mexico rings requires much more data than is now available.

For the present model the total velocity (u, v) of a drifter is composed of the translation velocity (U_T, V_T) of the ring center and the swirl velocity (u_S, v_S):

$$u = U_T + u_S$$
$$v = V_T + v_S \tag{1}$$

$$u_S = (d + a)x/2 + (b - c)y/2$$
$$v_S = (b + c)x/2 + (d - a)y/2 \tag{2}$$

Here x and y are the instantaneous coordinates, relative to the ring center of a particular parcel (drifter). If (2) is regarded as a Taylor expansion for the velocity field, then the parameters a and b can be interpreted as deformation rates and c and d as the vertical vorticity and horizontal divergence. It is stressed that these parameters are evaluated along individual paths. Eulerian estimates of deformation rates, vorticity, and divergence likely would differ from these estimates. Consequently, it is better to interpret a, b, and c as shape functions which determine the orientation and ellipticity of a particular orbit in a ring. See Kirwan et al. [1984b] for details.

The general solution to (1) and (2) is easily obtained [Okubo, 1970]. The procedure here is to apply this solution to every time interval between fixes (in practice, interpolated positions). Thus for the interval $t_k \leq t \leq t_{k+1}$, one obtains

$$u_k = U_{Tk} + (d_k + a_k)x_k/2 + (b_k - c_k)y_k/2 \tag{3}$$
$$v_k = V_{Tk} + (b_k + c_k)x_k/2 + (d_k - a_k)y_k/2 \tag{4}$$

where

$$x_k = \{\exp [r_{1k}(t - t_k)][X_k(\sqrt{a_k^2 + b_k^2 - c_k^2} + a_k) + Y_k(b_k - c_k)]$$
$$- \exp [r_{2k}(t - t_k)][X_k(a_k - \sqrt{a_k^2 + b_k^2 - c_k^2}) + Y_k(b_k - c_k)]\}$$
$$- 2\sqrt{a_k^2 + b_k^2 - c_k^2} \tag{5}$$

$$y_k = \{\exp [r_{1k}(t - t_k)][X_k(b_k + c_k) + Y_k(\sqrt{a_k^2 + b_k^2 - c_k^2} - a_k)]$$
$$+ \exp [r_{2k}(t - t_k)][- X_k(b_k + c_k) + Y_k(\sqrt{a_k^2 + b_k^2 - c_k^2} + a_k)]\}$$
$$- 2\sqrt{a_k^2 + b_k^2 - c_k^2} \tag{6}$$

In (5) and (6), (X_k, Y_k) are the coordinates of the parcel in question at time $t = t_k$ relative to the ring center. Also,

$$r_{1k} = (d_k + \sqrt{a_k^2 + b_k^2 - c_k^2})/2 \tag{7}$$
$$r_{2k} = (d_k - \sqrt{a_k^2 + b_k^2 - c_k^2})/2 \tag{8}$$

are the eigenvalues of the matrix

$$2M_k = \begin{bmatrix} (d_k + a_k) & (b_k - c_k) \\ (b_k + c_k) & (d_k - a_k) \end{bmatrix}$$

Note that these eigenvalues are complex conjugates when $c_k^2 > a_k^2 + t_k^2$. This, naturally, produces real periodic solu-

tions which are a characteristic of swirl velocities of drifters trapped in a ring.

To apply this model to drifter data, differentiate (3) and (4) three times with respect to time. One side of these equations contains the unknown variable set $Z_k = (a_k, b_k, c_k, d_k, X_k, Y_k)$. The other side of these equations can be estimated from path data. These six equations do not contain the translation velocity, since it is assumed a priori to be constant for a time interval. (But, of course, its value may change from one time interval to the next.) These six equations are inverted analytically for the six elements of Z_k. The translation velocities can be recovered from (3) and (4), since all other quantities are now known. Alternatively, the translation velocities can be obtained by differentiating the path of the ring center. Both procedures provide comparable estimates. Here we use the latter procedure. With all elements of Z_k now determined, one then moves to the next time interval and repeats the calculations, thus obtaining a time series of Z_k. Details are given in the appendix.

We have expended a great deal of effort in learning how to make reliable time derivative estimates of the path data. For the data analyzed here, the raw position files have been edited, interpolated to equally spaced time intervals, and low-pass filtered (half power point of 100 hours). All derivative estimates were obtained by fourth-order accurate, centered difference schemes. Each derivative file was edited and low-pass filtered. The calculations, as described in the appendix for Z_k, were performed with the latter derivative files. The calculated Z_k, in turn, were edited and low-pass filtered.

The analysis procedure just outlined is an improvement over that used by *Kirwan et al.* [1984b]. Their method required an a priori assignment of a solution form to (4) and (5); i.e., (7) and (8) were assumed to be complex conjugates, and values of Z_k were assumed to be constant over one ring revolution (approximately 15 days). The procedure used here does not require an a priori assignment of the solution form; it lets the data determine this. Thus it should have wider utility. In addition, the Z_k are now required to be constant over seven time intervals (42 hours in the present case) rather than 2 weeks.

As was indicated above, a, b, and c are not especially useful for comparison with Eulerian data. For rings a more appropriate description would be the elliptical structure of the orbit traversed by a particular drifter. As was shown by *Kirwan et al.* [1984b], the characteristic equation is

$$(c_k + b_k)x_k^2 + (c_k - b_k)y_k^2 - 2a_k x_k y_k$$
$$= L_k \exp\left[-d_k(t - t_k)\right] \quad (9)$$

Here L_k is the angular momentum per unit mass relative to the ring center. This can be calculated directly (see equation (A18)). In (9) the argument in the exponential term can be made zero by making the evaluation at the beginning of the time interval $t = t_k$. Note that a requirement for (9) to describe an ellipse is that $c_k^2 > a_k^2 + b_k^2$.

From analytic geometry it is known that for anticyclonic motion, $c_k < 0$, the major axis of the ellipse makes an angle with east of

$$\alpha_k = \tfrac{1}{2}\tan^{-1}\left(-a_k/b_k\right) \quad (10)$$

In evaluating (10), care must be exercised in the quadrant assignment. Also, the semilength of the major axis is

$$R_k = \sqrt{L_k/(c_k - h_k)} \quad (11)$$

where

$$h_k^2 = a_k^2 + b_k^2$$

The paradigm just outlined for analysis of Lagrangian data puts critical emphasis on time derivatives of path data. Inconsequential errors in the path data can become consequential in the derivative estimates. Moreover, the nonlinear algebraic combinations of these derivatives in the paradigm may magnify further the impact of these errors on the inversion. The concern is that two paths which contain the same kinematic information but differ by small random and/or round off errors, will produce vastly different kinematic estimates when run through the paradigm. The internal consistency of estimates of ring kinematics is presently being examined with simulated data from the HT GCM.

3. MIDGULF

3.1. *Observations*

Here the results of the intraring and inter-ring comparisons are presented for the midgulf region. This includes ring kinematics as inferred from the three drifters in the 1980–1981 ring and the single drifter in the 1982–1983 ring. While in the midgulf region, both rings began to interact with the continental slope topography and/or circulation. This period is isolated in the analysis. The same analysis routine is then applied to simulated midgulf ring data from the HT GCM.

The 1980–1981 ring. The data for this portion of the study come from three drifters (1598, 1599, and 1600) which were seeded in the 1980–1981 ring. *Kirwan et al.* [1984a, b] have already reported on this. The data have been reanalyzed using the general algorithm discussed in the preceding section and in the appendix.

Figure 2 shows the paths of these three drifters in the midgulf region along with the positions of the centers and the orbit ellipses. Arrows on the drifter and center paths mark 10-day intervals, while the ellipses are presented at 15-day intervals. The paths for each drifter are for a common time interval (day 340, 1980, to day 118, 1981). This figure establishes three points. First, all three make the same swath through this portion of the gulf, suggesting that they generally followed the ring. The overall path characteristics of drifters 1598 and 1600 (Figures 2a and 2c) are remarkably similar, suggesting that they were in very similar orbits. Second, the paths for the center of the ring, as determined independently from the three drifters, is in good agreement as far as about 94°W (the first 2 months of the record). Discounting the very beginning where there are numerical problems, the typical difference in the location of the center at any one time is 30 km, about 20% of the diameter of the ring as determined from satellite imagery [*Kirwan et al.*, 1984b]. This is about 10 km larger than the rms displacement between the maximum surface and interface displacement anomalies of the HT GCM. The 30-km variability is considerably larger than that reported by *Hooker and Olson* [1984] using a variant of the technique employed here under ideal conditions. In view of our results along the continental slope, described below, it is not clear whether the large variability is due to data, technique, or rapid evolution of the ring.

Finally, the ellipses also show generally good agreement east of 94°W. Note the tendency to develop a northwest elon-

gation as the ring approaches 94°W West of 94°W, all three orbits suggest that the ring begins to interact with the continental slope circulation and/or topography. This is discussed later.

Figure 3 shows the time series for the swirl and translation velocities. All three records indicate swirl velocities in excess of 50 cm s throughout most of the record. The dominant period is about 14 days with a variation of about 2 days between the records. This is recognized as the ring's rotation period. However, from about day 30 to 60, 1981, all three drifters show a smaller-period component (about 5 days) in the time series and a decrease in swirl amplitude. As will be discussed below,

Fig. 2a

Fig. 2b

Fig. 2c

Fig. 3a

Fig. 3b

Fig. 3c

Fig. 2. Drifter paths, inferred center path (red) and orbit ellipse (blue) for the three drifters in the 1980–1981 ring: (a) 1598, (b) 1599, and (c) 1600. Arrows on the paths are at 10-day intervals, while the ellipses are shown at 15-day intervals. Here S and F refer to start and finish.
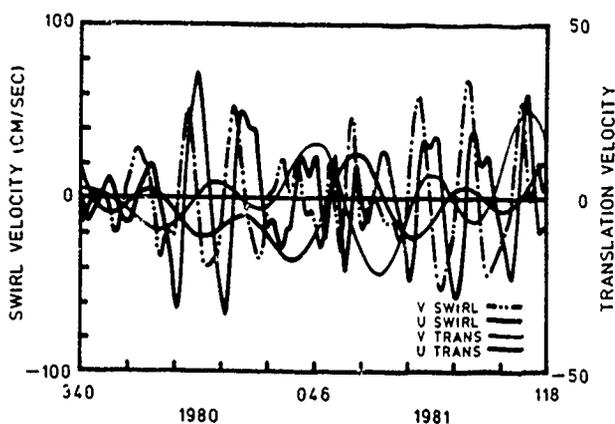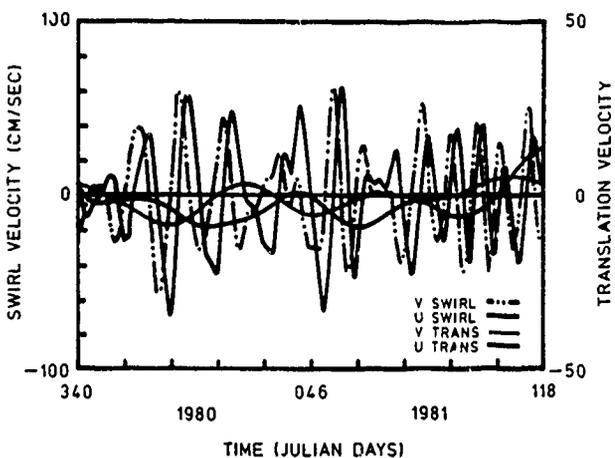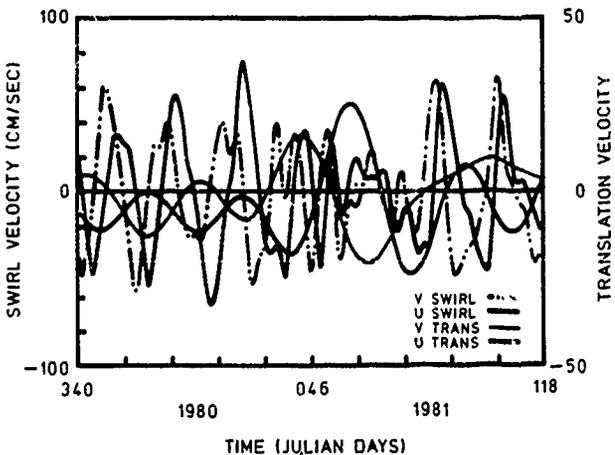
Fig. 3. Swirl (left scale) and translation velocities (right scale) inferred from the three drifters in the 1980–1981 ring. (a) 1598, (b) 1599, and (c) 1600. The east and north components of the translation velocity are depicted in red and blue, respectively.

it is speculated that during this period the drifters were responding to effects produced by the continental slope and/or circulation further to the west. All the translation velocities show a consistent westward component of about 4 cm/s up until about day 30, 1981. For the reason just given, it is not clear that the analysis applies to this ring for the period from day 30, 1981, to day 60, 1981 After day 60, 1981, the ring centers appear to be stationary.

The 1982 1983 ring and comparison with the 1980-1981 ring. The same characteristics are seen in the analysis for the 1982-1983 ring. Figure 4 shows the drifter path, inferred center path, and the orbit ellipses for drifter 3374. As in Figure 2, there is significant distortion of the orbits west of 94°W. Unlike the earlier ring, no significant northwest ellipticity is developed as the ring approaches 94°W. Comparison with Figure 2 indicates that the 1982-1983 ring center followed nearly the same path as that of the 1980-1981 ring.

swirl velocities decrease significantly and show some evidence of higher-frequency components. This is the period when the drifter moves west of 94°W and executes the deformed, northwest-oriented loop. As with the earlier ring, this is interpreted as evidence for topographic and/or slope circulation interactions.

Figure 2 indicates that west of 94°W, the three drifters in the 1980-1981 ring show significant divergence in the calculation of the inferred center Furthermore, drifters from both rings showed anomalous path characteristics in this region. In particular, 1598 and 1600 appeared to become entrained in smaller, anticyclonic eddies, while 1599 and 3374 exhibited warped and elongated ellipses. This has been attributed to interaction between the ring and the continental slope and/or slope circulation further to the west.

Figure 6 focuses on this time interval. Figure 6a shows the paths of all four drifters during the period in question. It is clear from this that all four drifters were under the influence of different dynamical processes here than those they experienced to the east.

Fig. 4. Drifter path, inferred center path (red), and orbit ellipse (blue) for the drifter in the 1982-1983 ring. Arrows on the paths are at 10-day intervals, while the ellipses are shown at 15-day intervals.

Fig. 6a

Fig. 5. Swirl (left scale) and translation velocities (right scale) inferred from the three drifters in the 1982-1983 ring. The east and north components of the translation velocity are depicted in red and blue, respectively.

Fig. 6b

Fig. 6. Paths of drifters 1598, 1599 and 1600 in the 1980-1981 ring and 3374 in the 1982-1983 ring for the period when they were interacting with the slope topography and/or circulation. The arrows are at 10-day intervals. (a) Drifter paths. (b) Inferred centers of flow.

Figure 5 shows the translation and swirl velocities for the 1982-1983 ring. The swirls are slightly less than 50 cm/s, which could reflect a smaller orbit of the drifter. The dominant period is still about 14 days. Note that around day 1, 1983 the

Figure 6b compares the movement of the inferred centers. In interpreting this figure, it should be emphasized that the center calculation is greatly complicated by the changes in curvature of the paths. The paradigm interprets this as a

change from an anticyclonic to cyclonic structure with a consequent change in the location of the center. No doubt the real dynamics during this period are much more complicated than the rather simple scenario available from the kinematic model. The geographic variation in the paths clearly is much larger than that seen east of 94°W or, as will be seen shortly, than that found along the slope. This suggests that each of these drifters was either briefly pulled out of the parent ring or its orbits deformed through interaction with the continental slope topography or circulation. This hypothesis accounts for the deformed orbits and the brief occurrence of high frequencies in the swirl velocities.

3.2. Simulations

Attention is now turned to the simulated data. There are two issues involved in the utilization and interpretation of this data. First, how consistent is the paradigm in recovering ring kinematics which should be independent of the orbit? This issue is presently being addressed. Addressed here is the issue of establishing how well the GCM agrees with the observations. Specifically, the center path, orbit ellipses, and translation velocity as inferred from the simulated data are compared with the same properties as determined from the observations.
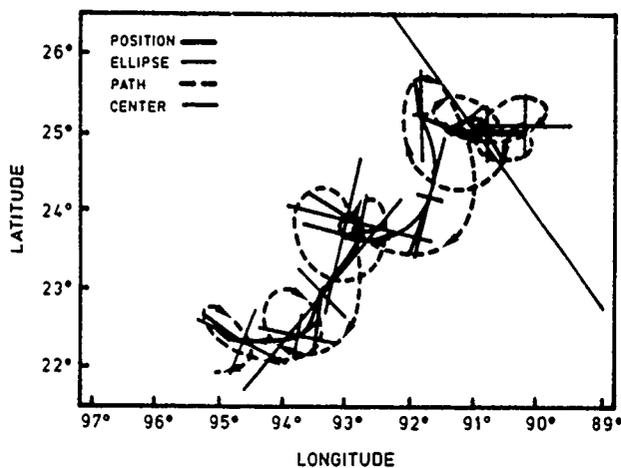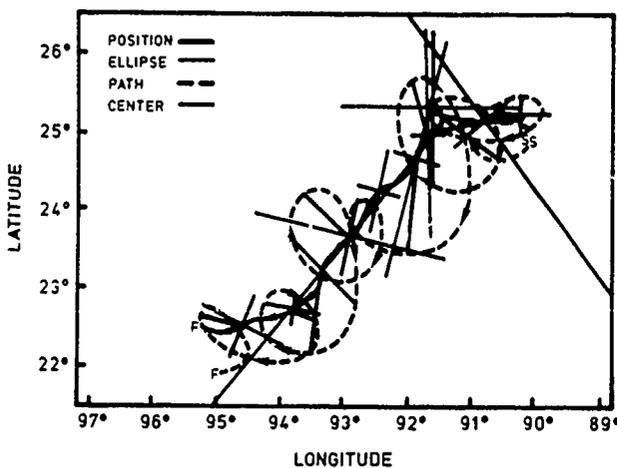
Figure 7 shows the path of one of several simulated drifters from the HT GCM along with the orbit ellipses. Figure 7a depicts the results using the ring center as inferred from the drifter orbit, while Figure 7b repeats the ellipse calculation using the position of the maximum displacement anomaly of the interface. The choice of the interface displacement as representative of the ring center is arbitrary. Presently, we are comparing the maximum interface displacement, the maximum surface elevation displacement and orbit-determined centers. In general, all are within 30 km of each other.

The most significant difference between the orbit-determined centers and interface displacement anomaly occurs in the interval between 91°W and 93°W where the orbit-inferred ring center shows a significant southern loop. This is not seen in the path of the maximum interface displacement anomaly. At 93°W the orbit-inferred center executes an anticyclonic loop that, again, is not seen in the displacement anomaly path. Elsewhere, the orbit-determined path is consistently 5 to 25 km south of the displacement anomaly path.

A comparison of Figures 2, 4, and 7 shows that the simulated and observed centers follow the same general path through this part of the midgulf. In general, the simulated center path is 10 to 35 km south of the observed path, depending upon which of the two simulated center paths is used. There is virtually no evidence of the interaction with the continental slope topography and circulation in the model results as was seen in the observations. None of the simulated orbits were deformed or appeared to be pulled out temporarily from the ring. Somewhat surprisingly, we have found less consistency in the ellipse calculations for the simulations than in the observations. A number of the ellipses from the simulated data are quite deformed. They also show frequent reversals of the major and minor axes. Overall, however, as the ring nears the slope region, a northeast orientation appears to develop in the orbit ellipses.

Figure 8 shows the translation and swirl velocities for the simulation. Figure 8a gives the results using the orbit center, and Figure 8b uses the maximum displacement anomaly as the ring center. The dominant period in the swirl velocities is about 24 days, or 10 days more than was found in the observations. Note that the swirl velocities, as calculated from either center, are of comparable magnitude, about 30 cm/s.

Fig. 7a

Fig. 7b

Fig. 8a

Fig. 7. Path and orbit ellipses (blue) of a simulated drifter from the HT GCM. Arrows on the path are at 10-day intervals, while ellipses are shown at 15-day intervals. Figure 7a shows the ellipses using the orbit-inferred center as the flow center, and Figure 7b uses the maximum interface displacement anomaly. Both centers are shown in red.
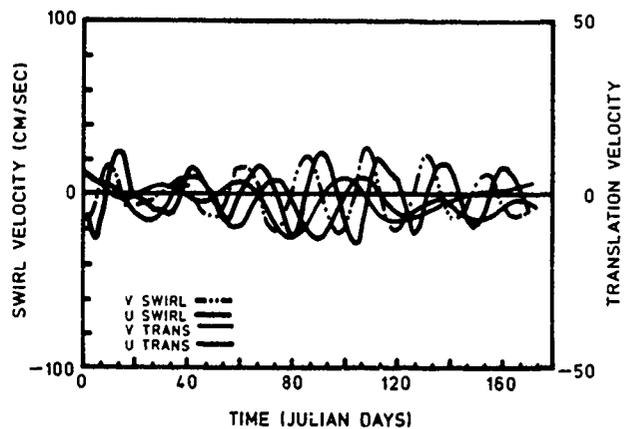
Fig. 8. Translation and swirl velocities as inferred from the HT GCM. The east and north components of the translation velocity are depicted in red and blue, respectively. The scale for the translation velocity is on the right. Figure 8a shows results using the orbit-inferred center, while Figure 8b (next page) shows results using the maximum displacement anomaly as the flow center.
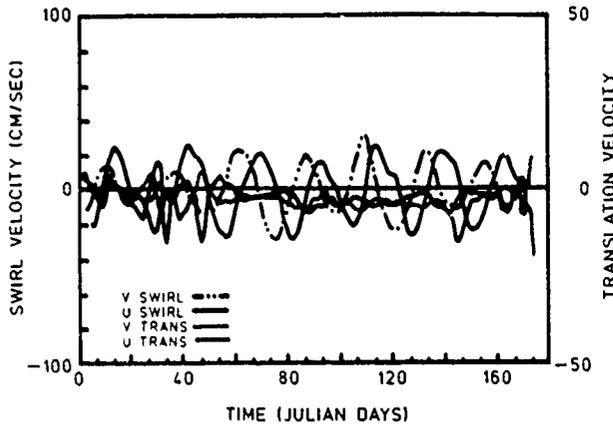
Fig. 8b

This is somewhat less than the observed swirls, but this could be rectified by picking a simulated drifter in a greater orbit. There seems to be more difference in the translation velocities. Because its path is straighter, the displacement anomaly path has less variance. The mean westward component in both cases of about 5 cm/s is consistent with the observations.
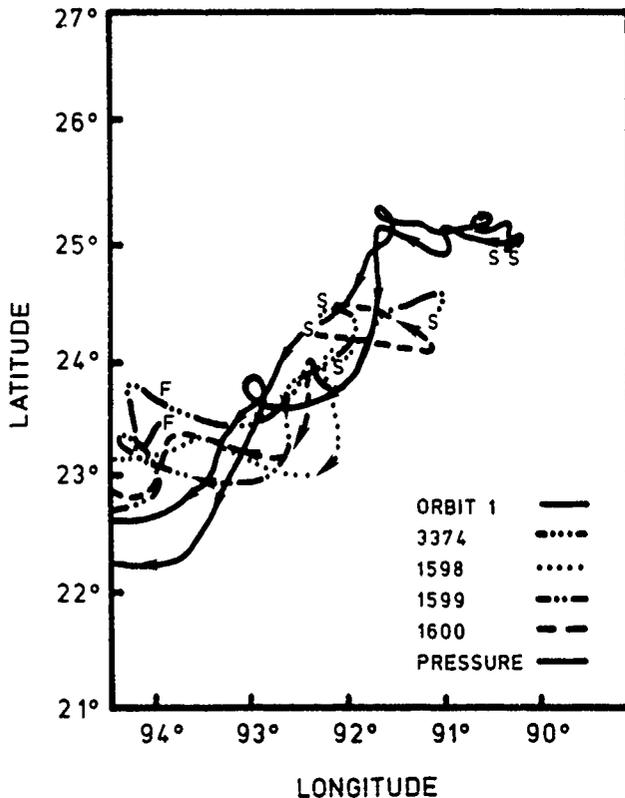
Fig. 9. The centers for the 1980–1981 ring, the 1982–1983 ring, and the HT GCM simulation. Orbit 1 (red) refers to the orbit-determined center, and pressure (blue) refers to the maximum displacement anomaly path. Arrows depict 10-day intervals.

Figure 9 compares the inferred center movement for all four drifters along with the inferred center of the simulated drifter and the displacement anomaly path east of 94°W. This is the region where there is no apparent effect of slope topography or circulation in the observations. Of course, details in the paths vary, but overall the agreement is quite good. The maximum deviation at any one time between any of the paths is

100 km, which is only two-thirds the diameter of a typical ring. For most of the paths, the orbit-determined centers are somewhat south of the displacement anomaly path. However, as the paths near 94°W, the observed centers move north of the displacement anomaly. All the orbit-determined center paths show considerably more structure than does that of the displacement anomaly.

4. CONTINENTAL SLOPE

It is remarkable that both observed rings and the simulated ring impacted the continental slope in the same area. This is seen in Figure 10, which shows the drifter paths, inferred center paths, and orbit ellipses for all three cases. In the case
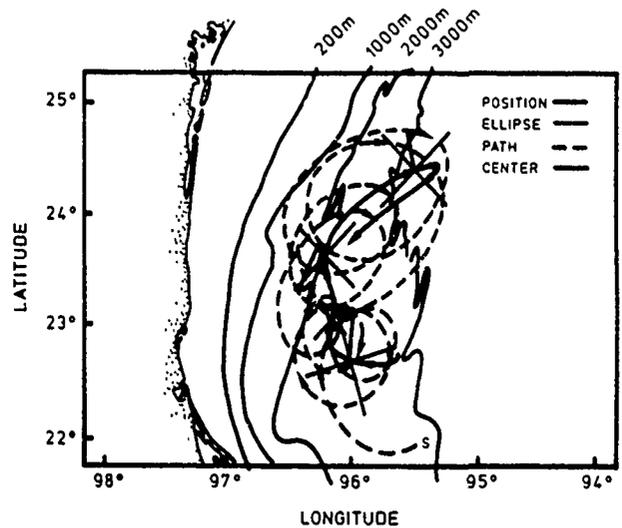
Fig. 10a
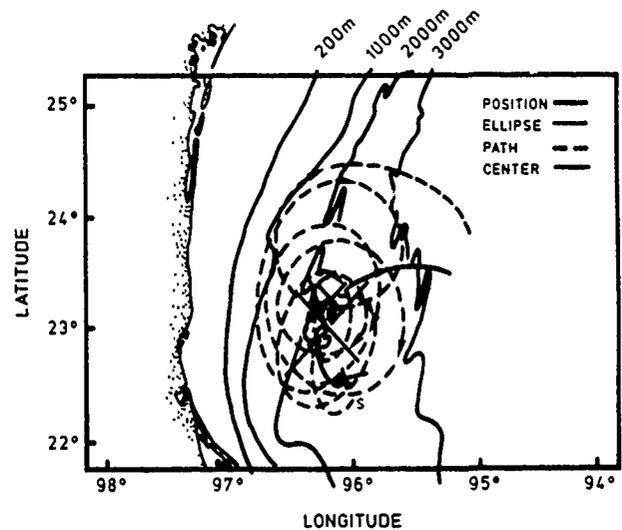
Fig. 10b

Fig. 10. Drifter paths, inferred centers and orbit ellipses for (a) the 1981–1982 ring, (b) the 1982–1983 ring (above); (c) the simulated ring, and (d) center paths along the continental slope (next page). Arrows on the paths depict 10-day intervals, while the ellipses are at 15-day intervals.

of the simulated data (Figure 10c), the orbit-inferred center path and the displacement anomaly path are virtually identical. Consequently, it is only necessary to display one set of calculations. The orbit-determined centers were used here.

Figure 10d illustrates how close the movements of the two observed and simulated rings are. There the paths of the inferred centers along with the displacement anomaly path have

been superimposed. Except for the beginning and end of the paths, the maximum deviation is 70 km with a rms deviation of 12 km. Moreover, all paths show the same general characteristics. Both the observations and simulation show a northward migration along the isobaths but with some eastward or looping component.

a decrease in the dominant period to about 15 days. The magnitudes of the observed ring's swirl velocities are about 40 to 50 cm/s, which is close to that found in the midgulf. The swirl velocity for the simulated ring is about 80 cm/s, substantially more than what was obtained for the midgulf. All translation velocities indicate a fairly steady northward movement of about 4 cm/s.

Fig. 10c

Fig. 11a

Fig. 10d

Fig. 10. (cont.) Drifter paths, inferred centers and orbit ellipses for (c) the simulated ring, and (d) center paths along the continental slope. Arrows on the paths depict 10-day intervals, while the ellipses are shown at 15-day intervals.

The northward migration along the slope is puzzling, as conventional theory [Smith and O'Brien, 1983] would have topographic beta drive the rings to the south. Recently, Smith [1986] has suggested that the northward migration may be due to boundary effects. An alternate explanation was offered by Nakamoto [1986], who found northward propagating soliton solutions in a two-layer, nonlinear, quasi-geostrophic model.

The swirl and translation velocity time series are shown in Figure 11. In the 1980–1981 ring the dominant period is 15 days, almost exactly that found in the midgulf. For the 1982–1983 ring the dominant period is about 11 days, slightly less than that found in the midgulf. The simulated ring also shows

Fig. 11b

Fig. 11c

Fig. 11. Swirl (left scale) and translation velocities (right scale) for the (a) 1980–1981, (b) 1982–1983, and (c) simulated rings along the continental slope.

5. CONCLUSIONS

The paths, translation and swirl velocities, and orbit ellipses have been calculated from Lagrangian observations for two large anticyclonic, Gulf of Mexico rings and one simulated ring. Within the capabilities of the data base and the analysis routine, the following are now established.

1. The paths of the three rings across the central Gulf of Mexico to the continental slope off of Mexico are virtually identical. However, not all Loop Current rings will follow this path. See *Lewis and Kirwan* [1987].

2. The intraring variability of translation and swirl velocities and the inferred center paths for the 1980–1981 ring are essentially the same as the inter-ring variability between the 1980–1981 and 1982–1983 rings.

3. For the observed rings, there was evidence of strong ellipticity developing as these rings approached the continental slope. The axis of orientation was approximately NE-SW. No independent data on ellipticity were available for the 1982–1983 ring, so it cannot be ruled out that this ring was so orientated. Similar but less pronounced ellipticity was seen in the simulated ring.

4. Both observed rings showed significant distortion of the drifter orbits west of 94°W. This is attributed to interaction of these rings with the continental slope topography and/or slope circulation features. Such interaction was not observed in the simulated ring.

5. After encountering the continental slope off of Mexico, both observed and simulated rings retained their integrity for at least several months while they migrated to the north. The track of the center of both was very close to the 1200-m isobath. The observed swirl speeds were slightly changed from the values obtained from the midgulf. The simulated ring exhibited a substantial increase in swirl velocity. For both the observed and simulated data, the translation speeds were comparable to those obtained for the midgulf.

There are a couple of broader implications of this study pertinent to eddy-resolving GCM's. Both the volume of data as well as the time and space scale resolution of simulated data available from these models far surpasses the typical observational data bases used for verification. Because of the different time and space scales of resolution in the simulated and observed data bases, it is not clear how to establish reliable criteria for statistical comparisons. This study suggests that a potent alternative is to compare model and observed Lagrangian kinematics. Both simulated and observed Lagrangian data sets provide comparable space-time resolution on the evolution of specific circulation features. Moreover, the assessment of the prediction of such features is a more stringent test of a model's predictive capability than are general statistics. The Lagrangian data also provide a means of fine-tuning model parameters such as layer depth, density differences, etc., so that observed and simulated swirl velocities can be matched. As to the HT model, this study has documented the interesting situation that the prediction improves in time, at least as far as the movement of the ring is concerned.

The second and related issue is the use of Lagrangian observations for updating prognostic models. In character, such data are similar to sea surface topographic data derived from satellites [see *Hurlburt*, 1986; *Thompson*, 1986; *Kindle*, 1986]. The Lagrangian data contain information on the motion of representative parcels but no information on what is happening nearby. Satellite topographic data return information just along the satellite path but give no information on the actual motion. Supplementing the latter data with the former data in eddy-resolving general circulation models could significantly upgrade their predictive capabilities.

APPENDIX

The purpose here is to provide some details on the inversion of (3) and (4) to obtain the time series for the elements of Z_k. The basis for this inversion is a Taylor expansion in time about the instant t_k of the velocity vector. From the left-hand side of (3) and (4) one obtains

$$u(t) = u(t_k) + u'(t_k)(t - t_k) + u''(t_k)(t - t_k)^2/2$$
$$+ u'''(t_k)(t - t_k)^3/6 \quad (A1)$$

$$v(t) = v(t_k) - v'(t_k)(t - t_k) + v''(t_k)(t - tk)^2/2$$
$$+ v'''(t_k)(t - t_k)^3/6 \quad (A2)$$

for the interval $t_k \leq t \leq t_{k+1}$. The primes represent time derivatives. Now each of the terms on the right-hand side of (A1) and (A2) can be estimated from the velocity record. For example $u(t_k)$ and $v(t_k)$ are merely the velocities at time t_k. The derivatives can be estimated by a variety of techniques; here we have employed centered finite differences.

Now the analytic solution, (5) and (6), can be expanded in a Taylor series as well. When this is done and coefficients of the appropriate powers in this expansion and (A1) and (A2) are equated, a system of simultaneous nonlinear equations is obtained for each time interval. With the subscript k suppressed, these are

$$X(a + d) + Y(b - c) + 2U_T = 2u \quad (A3)$$

$$X(b + c) + Y(d - a) + 2V_T = 2v \quad (A4)$$

$$X[(d + a)^2 + b^2 - c^2] + 2Yd(b - c) = 4u' \quad (A5)$$

$$2Xd(b + c) + Y[(d - a)^2 + b^2 - c^2] = 4v' \quad (A6)$$

$$X[(d + a)^3 + (b^2 - c^2)(3d + a)]$$
$$+ Y(b - c)(3d^2 + a^2 + b^2 - c^2) = 8u'' \quad (A7)$$

$$X(b + c)(3d^2 + a^2 + b^2 - c^2)$$
$$+ Y[(d - a)^3 + (b^2 - c^2)(3d - a)] = 8v'' \quad (A8)$$

$$X[(a^2 + b^2 - c^2 + d^2)^2 + 4d^2(a^2 + b^2 - c^2)$$
$$+ 4ad(a^2 + b^2 - c^2 + d^2)]$$
$$+ 4Yd(b - c)(a^2 + b^2 - c^2 + d^2)] = 16u''' \quad (A9)$$

$$4Xd(b + c)(a^2 + b^2 - c^2 + d^2) + Y[(a^2 + b^2 - c^2 + d^2)^2$$
$$+ 4d^2(a^2 + b^2 - c^2) - 4ad(a^2 + b^2 - c^2 + d^2)] = 16v''' \quad (A10)$$

These eight equations are inverted at each time step for X, Y, U_T, V_T, a, b, c, and d. To our surprise it seems that this can be done analytically. The key to this is the observation that the geometric invariants of the matrix M_k, i.e., Tr (M) and det (M), can be calculated from observations without knowing a, b, or c, a priori. After 3 years of inspection it was seen that

$$\det (M) = 2(u''v''' - u'''v'')/(u'v'' - v'u'') = M^2 \quad (A11)$$

$$\text{Tr } (M) = (u'v''' - v'u''')/(u'v'' - v'u'') = d \quad (A12)$$

Insertion of M^2 and d, calculated from (A11) and (A12), respectively, into (A5)–(A10) significantly simplifies the latter

expressions. Considerable routine algebra then yields

$$X = 8[u'(M^2 + 2d^2) - 2u''']/M^4 \qquad \text{(A13)}$$

$$Y = 8[v'(M^2 + 2d^2) - 2v''']/M^4 \qquad \text{(A14)}$$

$$a = -\{K_1 M^2 + K_2 + K_3(d/2)\}/N \qquad \text{(A15)}$$

$$b = \{H_1 M^2 + H_2 + H_3(d/2)\}/N \qquad \text{(A16)}$$

$$c = -\{G_1 M^2 - G_2 + G_3(d/2)\}/N \qquad \text{(A17)}$$

where

$$N = 8(u'v'' - u''v');$$

$$G_1 = 2(u'^2 + v'^2);$$

$$G_2 = 8(u'^2 + v''^2);$$

$$G_3 = 16(u'u'' + v'v'');$$

$$H_1 = 2(u'^2 - v'^2);$$

$$H_2 = 8(u''^2 - v''^2);$$

$$H_3 = 16(u'u'' - v''v');$$

$$K_1 = 2u'v';$$

$$K_2 = 8u''v'';$$

$$K_3 = 8(u'v'' + u''v').$$

Incidentally, the parameter N is directly related to the angular momentum per unit mass of the orbit L:

$$L = -4N/M^4 \qquad \text{(A18)}$$

The final step in the calculations is to determine the translation velocities from (A3) and (A4). This is trivial, since all other terms are now known.

REFERENCES

Austin, G. B., Some recent oceanographic surveys of the Gulf of Mexico, *EOS Trans. AGU, 36*(5), 885–892, 1955.

Blaha, J. P., and W. Sturges, Evidence for wind forced circulation in the Gulf of Mexico, technical report, Dep. of Oceanogr., Fla. State Univ., Tallahassee, 1978.

Elliot, B. A., Anticyclonic rings and the energetics of the circulation of the Gulf of Mexico, Ph.D. dissertation. Tex. A&M Univ., College Station, 1979.

Elliot, B. A., Anticyclonic rings in the Gulf of Mexico, *J. Phys. Oceanogr., 12*, 1293–1309, 1982.

Flierl, G. R., Particle motions in large amplitude wave fields, *Geophys. Astrophys. Fluid Dyn., 18*, 39–74, 1981.

Hooker, S. B., and D. B. Olson, Center of mass estimation in closed vortices: A verification in principle and practice, *J. Atmos. Oceanic Technol., 1*(3), 247–255, 1984.

Hurlburt, H. E., Dynamic transfer of simulated altimeter data into subsurface information by a numerical ocean model, *J. Geophys. Res., 91*(C2), 2372–2400, 1986.

Hurlburt, H. E., and J. D. Thompson, A numerical study of Loop Current intrusions and eddy shedding, *J. Phys. Oceanogr., 10*, 1611–1651, 1980.

Ichiye, T., Circulation and water mass distribution in the Gulf of Mexico, *Geofis. Int., 2*, 47–76, 1962.

Kindle, J. C., Sampling strategies and model assimilation of altimetric data for ocean modeling and prediction, *J. Geophys. Res., 91*(C2), 2418–2432, 1986.

Kirwan, A. D., Jr., A note on a geophysical fluid dynamics variational principle, *Tellus, Ser. A, 36*, 211–215, 1984.

Kirwan, A. D., Jr., W. J. Merrell, Jr., J. K. Lewis, and R. E. Whitaker, Lagrangian observations of an anticyclonic ring in the Western Gulf of Mexico, *J. Geophys. Res., 89*, 3417–3424, 1984a.

Kirwan, A. D., Jr., W. J. Merrell, Jr., J. K. Lewis, R. E. Whitaker, and R. Legeckis, A model for the analysis of drifter data with an application to a warm core ring in the Gulf of Mexico, *J. Geophys. Res., 89*, 3425–3428, 1984b.

Lewis, J. K., and A. D Kirwan, Jr., Some observations of ring-topography and ring-ring interactions in the Gulf of Mexico, *J. Geophys. Res., 90*(C5), 9017–9028, 1985.

Lewis, J. K., and A. D. Kirwan, Jr., Genesis of a Gulf of Mexico ring as determined from kinematic analyses, *J. Geophys. Res., 92*(C11), 11,727–11,740, 1987.

Nakamoto, S., Application of solitary wave theory to mesoscale eddies in the Gulf of Mexico, Ph.D. dissertation, 50 pp., Dep. of Oceanogr., Tex. A&M Univ., College Station, 1986.

Nowlin, W. D., *Winter Circulation Patterns and Property Distributions, Tex. A&M Univ. Oceanogr. Stud.,* vol. 2, edited by L. R. A. Capurro and J. L. Reid, pp. 3–53, Gulf, Houston, Tex., 1972.

Nowlin, W. D., and H. J. McClellan, A characterization of the Gulf of Mexico waters in winter, *J. Mar. Res., 25*, 29–59, 1967.

Okubo, A., Horizontal dispersion of floatable particles in the vicinity of velocity singularities such as convergences, *Deep Sea Res., 17*, 445–454, 1970.

Smith, D. C., IV, A numerical study of Loop Current eddy interaction with bottom topography in the western Gulf of Mexico, *J. Phys. Oceanogr., 16*(7), 1260–1272, 1986.

Smith, D. C., IV, and J. J. O'Brien, The interaction of a two layer isolated mesoscale eddy with topography, *J. Phys. Oceanogr., 13*, 1681–1697, 1983.

Smith, D. C., IV, and R. O. Reid, A numerical study of non-friction decay of mesoscale eddies, *J. Phys. Oceanogr., 12*(3), 244–255, 1982.

Sturges, W., and J. P. Blaha, A western boundary current in the Gulf of Mexico, *Science, 192*, 367–369, 1976.

Sweitzer, N. B., Jr., Origin of the Gulf Stream and circulation of waters in the Gulf of Mexico with special reference to the effect on jetty construction, *Trans. Am. Soc. Civ. Eng., 40*, 86–98, 1898.

Thompson, J. D., Altimeter data and geoid error in mesoscale ocean prediction: Some results from a primitive equation model, *J. Geophys. Res., 91*(C2), 2401–2417, 1986.

A. W. Indest and A. D. Kirwan, Department of Oceanography, Old Dominion University, Norfolk, VA 23508.

J. K. Lewis, Science Applications International Corporation, 1304 Deacon, College Station, TX 77480.

I. Quintero and P. Reinersman, Department of Marine Science, University of South Florida, 140 Seventh Avenue South, Saint Petersburg, FL 33701.

Notes on the Cluster Method for Interpreting Relative Motions

A. D. KIRWAN, JR.

Department of Oceanography, Old Dominion University, Norfolk, Virginia

It is shown that the so-called cluster method for determining the horizontal gradients of the horizontal velocity has some basic limitations caused by restrictive physical assumptions. For large-area clusters there is aliasing of these estimates by large-scale shear, while for small-area clusters, the displacement of the statistical cluster center from a physically significant flow center can produce seriously aliased cluster model parameter estimates. These effects are independent of typical experimental problems such as measurement error and statistical reliability. An alternative to the cluster paradigm is proposed. This, however, requires solving a nonlinear inverse problem to recover estimates of the horizontal velocity gradients.

INTRODUCTION

Estimates of the horizontal spatial derivatives of the near-surface, horizontal velocity are of obvious importance in a wide range of scales in ocean dynamics. They are notoriously difficult to obtain. Most estimates have come from relative motion analysis of drifter clusters. For an older summary of results, see *Kirwan* [1975]. *Fahrbach et al.* [1986] have recently applied this technique to drifter data from the equatorial Atlantic.

Sanderson et al [1988] have pointed out a statistical bias in using this technique if the number of drifters in the cluster is small. Of course, the statistical significance of model parameter estimates, as well as the effect of measurement errors in estimating the velocity gradient tensor, is important. There is, however, another problem with this technique. This is the tacit assumption that the center of mass of the cluster corresponds to the center of the flow field about which a Taylor's expansion of the velocity field can be made.

The purpose here is twofold. The first is to show that with the cluster paradigm, a deviation of the cluster center from a flow center can result in serious biases in gradient estimates. The other is to propose an alternative to the cluster model that avoids the center bias problem. The new approach provides independent estimates of the velocity gradient estimates; however, it requires solving a nonlinear inverse problem.

THEORY

The first part of the cluster paradigm is given by

$$(r_a^P - r_{oa}^P)/\Delta = u_a^P = U_a^\circ + \sum_b H_{ab} r_{ob}^P + r_a''^P/\Delta \quad (1)$$

Here Δ is the time difference between fixes, r_a^P is the a component of the position vector from the cluster center of mass to the drifter path, r_{oa}^P is its original or previous position vector, H_{ab} is the velocity gradient, and U_a° is a steady mean flow. Figure 1a is a cartoon of the general geometry. As has been noted by many previous investigators, (1) can be obtained by a Taylor's expansion of the velocity field.

The first term on the right-hand side of (1) is a uniform translation of the center, and the second term is a local swirl induced by a homogeneous deformation field. The last term in (1) is a residual, the minimization of which yields estimates of U_a° and H_{ab}. For the latter operation it is necessary to intro-

duce the cluster average of property h^P

$$\langle h^P \rangle = \sum h^P/N \quad (2)$$

where N is the statistical degrees of freedom in the cluster average and the sum is over all drifters in the cluster [see *Sanderson et al.*, 1988]. Note that by definition

$$\langle r_a^P \rangle = 0 \quad (3)$$

This is the second part of the cluster paradigm. It is stressed that (3) significantly constrains the basic assumption and validity of a two-term Taylor expansion.

By standard minimization augmented with (3), the least squares estimates of U_a° and H_{ab} are

$$U_a^\circ = \langle u_a^P \rangle \quad (4)$$

$$H_{ab} = \sum_i R_{bi} \langle u_a^P r_i^P \rangle \quad (5)$$

where

$$R_{\beta\gamma} = \langle (r_\beta^P r_\gamma^P) \rangle^{-1} \quad (6)$$

is the inverse of the statistical moment of inertia matrix of the cluster. Details and variations of (4) and (5) are given by *Molinari and Kirwan* [1975], *Okubo and Ebbesmeyer* [1976], and *Okubo et al.* [1976].

This model is critically dependent upon (1) a translation velocity U_a° common to all drifters, (2) a velocity gradient tensor H_{ab} common to all drifters, i.e., a homogeneous deformation field, and (3) equation (3).

In order to assess the role these assumptions play, consider a more general kinematic flow model:

$$u_a^P = V_a^P + \sum_b G_{ab}^P x_b^P + r_a''^P/\Delta \quad (7)$$

Here x_b^P is the position vector to the drifter path from a physically relevant local origin. This is called the flow center to distinguish it from the cluter center. See Figure 1a for the geometric relation between x_b^P and r_b^P. The latter depends upon the geometric characteristics of the drifter array; the former depends on true flow field characteristics. This model differs from (1) in that it allows for a separate Taylor's expansion for each drifter. Thus there are distinct translation velocites V_a^P, as well as distinct velocity gradients G_{ab}^P, for each drifter. Also in contrast to (3)

$$\langle x_b^P \rangle \neq 0 \quad (8)$$

It should be clear, however, that if the three assumptions listed in the preceding paragraph are imposed on (7), it will reduce to (1).
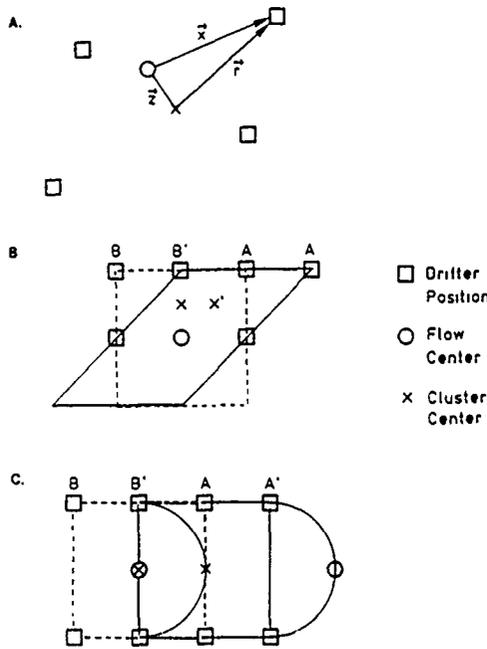
Fig. 1 Cartoon showing the essential geometry. (a) Basic vectors z, r, and x for the present configuration. (b) Displacements for case I. This could result from equal shear and normal deformation and anticyclonic rotation. The solid line indicates the present configuration, and the dashed line indicates the previous configuration. (c) Displacements for case II Initially, the cluster and flow centers coincide, but in the present (solid line) configuration the flow center has moved away from the cluster center. All panels depict the movement and deformation of the material lines connecting the drifters as well as a hypothetical array initially symmetric about the flow center.

Given only cluster data, the observables are $U_a{}^P$ and $r_a{}^P$. We now examine the effect of naively applying the cluster paradigm to this more general situation. Taking the cluster center as the local origin and letting

$$z_a{}^P = r_a{}^P - x_a{}^P \qquad (9)$$

be the displacement vector from the cluster center to flow center, it is deduced from (4), (5), (7), and (9) that

$$U_a{}^o = \langle V_a{}^P \rangle + \sum_b \langle G_{ab}{}^P(r_a{}^P - z_a{}^P) \rangle \qquad (10)$$

$$H_{ab} = \sum_\gamma R_{b\gamma}(\langle V_a{}^P r_\gamma \rangle + \sum_\delta \langle G_{a\delta}{}^P(r_\delta{}^P - z_\delta{}^P)r_\delta{}^P \rangle) \qquad (11)$$

These last two equations show that in general, the cluster model parameters are weighted averages of the flow model. In order for (10) and (11) to reduce to (4) and (5), all three assumptions given above must be made.

The following special cases illustrate the tenuous character of the cluster model.

Case I. There is no translation ($V_a{}^P \equiv 0$), and the deformation field is homogeneous; i.e., $G_{ab}{}^P$ is the same for all drifters ($G_{ab}{}^P = G_{ab}$). An example of this situation would be when the drifters are embedded in a flow field characterized by no translation and homogeneous vorticity and deformation fields (see Figure 1b). It is seen immediately from (10) and (11) that the cluster model will yield bogus parameter estimates of

$$U_a{}^o = - \sum_b G_{ab}\langle z_a{}^P \rangle \qquad (12)$$

$$H_{ab} = G_{ab} - \sum_\gamma R_{b\gamma} \sum_\delta G_{a\delta}\langle z_\delta{}^P r_\gamma{}^P \rangle \qquad (13)$$

The bogus translation velocity has the structure of a swirl

velocity and is of the order of the true velocity gradient times the distance between the two centers. For small area clusters, this displacement could well be of the cluster horizontal scale, and so the cluster determined translation velocity could be of the order of the swirl velocity. In the case of the velocity gradient estimate, there is no a-priori reason to expect $\langle z_\delta{}^P r_\gamma{}^P \rangle$ to be small; hence the "correction" term in (13) could be of the order of the correct value. As an aside, (13) is recognized as an extension of Pappas' theorem from mechanics.

Case II. The translation velocity varies from drifter to drifter; however, assumptions 2 and 3 hold (see Figure 1c). This case would include the situation where the drifters are deployed in a jet such as the Gulf Stream. Perhaps, fortuitously, the cluster center initially coincides with the flow center, say, the axis of the jet. The cluster parameter estimates now are

$$U_a{}^o = \langle V_a{}^P \rangle \qquad (14)$$

$$H_{ab} = G_{ab}{}^P + \sum_\gamma R_{b\gamma}\langle V_a{}^P r_\gamma{}^P \rangle \qquad (15)$$

If the flow center is indeed the jet axis, then the cluster model will yield a translation velocity for the center somewhat less than the maximum velocity of the jet as indicated by (14). Moreover, if the jet velocity is symmetric about the flow axis, then the cluster gradient estimates of the cluster scale velocity gradients will include an alias from the larger-scale shear across the jet as exemplified in the inhomogeneous nature of $V_a{}^P$ (the second right-hand side term in (15)). In general, the cluster model may not be able to distinguish between small-scale and large-scale shears.

These two cases highlight a basic difficulty of the cluster method. If the area covered by the cluster is small, there is a high likelihood that there will be a significant displacement between the cluster and flow centers. This is where case I applies. This can be alleviated by increasing the area extent of the cluster (with or without additional drifters), but then the large-scale shear may defeat the cluster model, as is indicated by the analysis in case II.

Case III. Only assumption 2 holds. In this case, the cluster parameter estimates will superpose (12) and (14) for $U_a{}^o$ and (13) and (15) for H_{ab}.

It is emphasized that the problems indicated above cannot be rectified by increasing the number of drifters and/or the cluster area and/or the position fix accuracy and frequency. The basic issue here is the weakness of the physics implied by the approach, not the accuracy or statistical significance of the measurements.

DISCUSSION

The preceding analysis suggests that the cluster method for estimating velocity gradients should be used with extreme caution. Other observations should be used to establish its applicability in specific experiments.

There is an alternative to the cluster paradigm for extracting velocity gradient information from path data. The alternative makes use of a kinematic model first proposed by Okubo [1970] and recently discussed by Perry and Chong [1987]. This approach makes use of the fact that (7) (and hence (1)) can be readily integrated to obtain particle paths. If the deformation field is homogeneous and stationary, then a single particle path contains the same information on the deformation as does a hypothetical cluster of nearby particles. The only characteristic difference in the paths is their starting positions.

To illustrate how the deformation information is contained

in the path data, it is necessary to calculate the path. Neglecting the last term in (7) and assuming that $V_a{}^P$ is steady in time, standard techniques yield

$$w_1{}^P(t) - W_1{}^{Po}(t_o) = V_1{}^P(t - t_o) + x_1{}^P(t) \qquad (16)$$

$$w_2{}^P(t) - W_2{}^{Po}(t_o) = V_2{}^P(t - t_o) + x_2{}^P(t) \qquad (17)$$

Here $w_a{}^P(t)$ is the absolute position at time t, and $W_a{}^{Po}(t_0)$ is the initial position of the flow origin at time t_o of drifter p.

The other quantities in (16) and (17) are

$$x_1{}^P(t) = \{\exp [m_+{}^P(t - t_o)][X_1{}^P(I^P + G^P) + X_2{}^P G_{12}{}^P]\}$$

$$- \{\exp [m_-{}^P(t - t_o)][X_1{}^P(G^P - I^P) + X_2{}^P G_{12}{}^P]\}/2I^P \qquad (18)$$

$$x_2{}^P(t) = \{\exp [m_+{}^P(t - t_o)][X_1{}^P G_{21}{}^P + X_2{}^P(I^P - G^P)]\}$$

$$+ \{\exp [m_-{}^P(t - t_o)][-X_1{}^P G_{21}{}^P + X_2{}^P(I^P + G^P)]\}/2I^P \qquad (19)$$

$$m_{+,-}{}^P = [Tr(G_{ab}{}^P) \pm I^P]/2 \qquad (20)$$

$$G^P = G_{11}{}^P - G_{22}{}^P \qquad (21)$$

$$I^P = \{(G^P)^2 + (G_{12}{}^P + G_{21}{}^P)^2 - (G_{12}{}^P - G_{21}{}^P)^2\}^{1/2} \qquad (22)$$

$$X_a{}^P = X_a{}^P(t_0) \qquad (23)$$

Given the path data, i.e., the left-hand side of (16) and (17) for a few intervals of time, the velocity gradient $G_{ij}{}^P$ and translation velocity $V_a{}^P$ can be estimated. This, however, is a problem in nonlinear parameter estimation and hence of more fundamental mathematical interest than purely linear statistical models. *Kirwan et al.* [1988] have provided one method of obtaining these estimates. Presumably, more efficient methods are available.

It is stressed that the estimates of the velocity gradient and translation velocity apply only to drifter p. Other drifters, if present, would supply independent estimates. This would allow statistical assessments of the uniformity of the flow field parameters.

A cautionary note on application of the proposed technique should be made. First, gradient estimates from this approach are truly Lagrangian, and so there may be some difficulty relating them to Eulerian estimates. Second, there are certain pathological situations where the deformation field will produce variability in only one of the velocity components. In these cases it may not be possible to recover all the gradient information. See *Okubo* [1970] and *Perry and Chong* [1987] for a complete discussion of pathological situations in critical points in flow fields.

REFERENCES

Fahrbach, E., C. Brockmann, and J. Meincke, Horizontal mixing in the Atlantic Equatorial Undercurrent estimated from drifting buoy clusters, *J. Geophys. Res., 91*(C9), 10,557–10,565, 1986.

Kirwan, A. D., Jr., Oceanic velocity gradients, *J. Phys. Oceanogr, 5,* 729–735, 1975.

Kirwan, A. D., Jr., J. K. Lewis, A. W. Indest, P. Reinersman, and I. Quintero, Observed and simulated kinematic properties of loop current rings, *J. Geophys. Res., 93*(C2), 1189–1198, 1988.

Molinari, R., and A. D. Kirwan, Jr., Calculations of differential kinematic properties from Lagrangian observations in the Western Caribbean Sea, *J. Phys. Oceanogr., 5,* 361–368, 1975.

Okubo, A., Horizontal dispersion of floatable particles in the vicinity of velocity singularities such as convergences, *Deep Sea Res., 17,* 445–454, 1970.

Okubo, A., and C. C. Ebbesmeyer, Determination of vorticity, divergence and deformation rates from analysis of drogue observations, *Deep Sea Res., 23,* 349–352, 1976.

Okubo, A., C. C. Ebbesmeyer, and J. M. Helseth, Determination of Lagrangian deformation from analysis of current followers, *J. Phys. Oceanogr., 6,* 524–527, 1976.

Perry, A. E., and M. S. Chong, A description of eddying motions and flow patterns using critical-point concepts, *Annu. Rev Fluid Mech, 19,* 125–155, 1987.

Sanderson, B. G., B. K. Pal, and A. Goulding, Calculations of unbiased estimates of the magnitude of residual velocities from a small number of drogue trajectories, *J. Geophys. Res., 93,* 8161–8162, 1988.

A. D. Kirwan, Jr., Department of Oceanography, Old Dominion University, Norfolk, VA 23529.